

1 **Amazonian trees have limited capacity to acclimate plant hydraulic properties in**  
2 **response to long-term drought**

3 **Running title: Hydraulic drought acclimation of Amazonian trees**

4  
5 Bittencourt P. R. L.<sup>1,2</sup>, Oliveira R. S.<sup>2,3</sup>, da Costa A. C. L.<sup>4</sup>, Giles A. L.<sup>2</sup>, Coughlin I.<sup>5,6</sup>,  
6 Costa P. B.<sup>2,3</sup>, Bartholomew, D.C.<sup>1</sup>, Ferreira L. V.<sup>7</sup>, Vasconcelos S. S.<sup>8</sup>, Barros, F.V.<sup>1,2</sup>,  
7 Junior J. A. S.<sup>2</sup>, Oliveira A. A. R.<sup>7</sup>, Mencuccini M.<sup>9,10</sup>, Meir P.<sup>6,11</sup>, Rowland L.<sup>1</sup>

8  
9 \*Corresponding Author: [paulo09d@gmail.com](mailto:paulo09d@gmail.com) (+44 07594951498), Amory Building,  
10 Department of Geography, College of Life and Environmental Sciences, University of Exeter,  
11 Exeter, UK, EX4 4RJ.

12  
13 <sup>1</sup>College of Life and Environmental Sciences, University of Exeter, Exeter, EX4 4RJ, UK

14 <sup>2</sup>Instituto de Biologia, University of Campinas (UNICAMP), Campinas, SP 13083-970, Brasil.

15 <sup>3</sup>Biological Sciences, UWA, Perth, WA, Crawley 6009, Australia

16 <sup>4</sup>Instituto de Geosciências, Universidade Federal do Pará, Belém, PA 66075-110, Brasil

17 <sup>5</sup>Departamento de Biologia, FFCLRP, Universidade de São Paulo, Ribeirão Preto, SP 14040-  
18 900, Brasil

19 <sup>6</sup>Research School of Biology, Australian National University, Canberra, ACT 2601 Australia

20 <sup>7</sup>Museu Paraense Emílio Goeldi, Belém, PA 66040-170, Brasil

21 <sup>8</sup>EMBRAPA Amazônia Oriental, 14 Belém, PA 66095-903, Brasil

22 <sup>9</sup>CREAF, Campus UAB, Cerdanyola del Vallés, 08193 Spain

23 <sup>10</sup>ICREA, Barcelona, 08010, Spain

24 <sup>11</sup>School of GeoSciences, University of Edinburgh, Edinburgh, EH9 3FF, UK

**25 Abstract**

26 The fate of tropical forests under future climate change is dependent on the capacity of their  
27 trees to adjust to drier conditions. The capacity of trees to withstand drought is likely to be  
28 determined by traits associated with their hydraulic systems. However, data on whether  
29 tropical trees can adjust hydraulic traits when experiencing drought remain rare. We  
30 measured plant hydraulic traits (e.g. hydraulic conductivity and embolism resistance) and  
31 plant hydraulic system status (e.g. leaf water potential, native embolism and safety margin)  
32 on >150 trees from 12 genera (36 species) and spanning a stem size range from 14 to 68 cm  
33 diameter at breast height (DBH) at the world's only long-running tropical forest drought  
34 experiment. Hydraulic traits showed no adjustment following 15 years of experimentally  
35 imposed moisture deficit. This failure to adjust resulted in these drought-stressed trees  
36 experiencing significantly lower leaf water potentials, and higher, but variable, levels of  
37 native embolism in the branches. This result suggests that hydraulic damage caused by  
38 elevated levels of embolism is likely to be one of the key drivers of drought-induced  
39 mortality following long-term soil moisture deficit. We demonstrate that some hydraulic  
40 traits changed with tree size, however, the direction and magnitude of the change was  
41 controlled by taxonomic identity. Our results suggest that Amazonian trees, both small and  
42 large, have limited capacity to acclimate their hydraulic systems to future droughts,  
43 potentially making them more at risk of drought-induced mortality.

44

45 **Key-words:** hydraulic traits; throughfall exclusion; Amazon rainforest; drought; embolism  
46 resistance; tropical forest, plant functional diversity; tree size.

## 47 **Introduction**

48           The responses of forested ecosystems to global changes in climate will partly depend  
49 on the capacity of forest trees to acclimate to new environmental conditions (Corlett, 2016;  
50 Galbraith *et al.*, 2010; Smith & Dukes, 2013; Sterck *et al.*, 2016). The Amazon forest is  
51 predicted to become warmer and drier over the coming decades (Duffy *et al.*, 2015; Lopes *et*  
52 *al.* 2016; Marengo *et al.*, 2018). This is likely to influence species composition, forest cover  
53 and the strength of the carbon sink (Malhi *et al.*, 2009; Phillips *et al.*, 2010), unless trees can  
54 fully or partially acclimate to survive and maintain function in the new conditions they face  
55 (Sterck *et al.*, 2016). Currently however, there is limited knowledge about the plasticity of  
56 traits in Amazonian trees and therefore their capacity to acclimate functionally to new  
57 environmental conditions, particularly drought. The few drought experiments constructed to  
58 date in tropical rainforests show some tree traits are plastic and respond to drought (Binks *et*  
59 *al.*, 2016; Schuldt *et al.*, 2011; Tng *et al.*, 2018). However, to our knowledge no studies exist  
60 which test the potential of tropical trees to adjust their hydraulic system to long-term drought,  
61 including traits indicating both hydraulic safety and efficiency (Meir *et al.*, 2018). As tree  
62 mortality is likely to be linked to the failure of a plant in controlling its hydraulic system  
63 status (Choat *et al.*, 2018; McDowell & Allen, 2015; Rowland *et al.*, 2015a), understanding  
64 the adjustment capacity of these traits will be vital for predicting future responses of tropical  
65 rainforests to changes in climate, particularly given the natural longevity of their constituent  
66 trees.

67           The plant hydraulic system is tightly linked to its water and carbon metabolism (Eller  
68 *et al.*, 2018; Christoffersen *et al.*, 2016) and therefore it is likely that plants require  
69 adjustments in their hydraulic system to maintain a positive carbon balance in the face of  
70 climate change. Several studies have shown plastic responses (variations in phenotype  
71 expression in response to environmental change) of leaf physiology and plant architecture to

72 experimental or natural drought (Ambrose, Sillett, & Dawson, 2009; Dayer *et al.*, 2017; Egea  
73 *et al.*, 2012; Prendin, Mayr, Beikircher, von Arx, & Petit, 2018; Yue *et al.*, 2019). Some  
74 studies also report plastic responses in hydraulic traits to short-term drought, related to both  
75 hydraulic safety and hydraulic efficiency (Awad, Barigah, Badel, Cochard, & Herbette, 2010;  
76 Beikircher & Mayr, 2009; Prendin *et al.*, 2018; Tomasella *et al.*, 2018). However, whether  
77 this plasticity can positively influence plant function (e.g. water stress status, photosynthesis,  
78 growth or reproduction) and can lead to partial or full acclimation in function is often hard to  
79 determine. As a working hypothesis, we define acclimation as a functional adjustment  
80 (which may be physiological, anatomical, or morphological) to maintain or enhance  
81 performance in response to new environmental conditions, similar to Way & Yamori (2014).  
82 Research on hydraulic acclimation in tropical trees in response to drought is limited as most  
83 drought experiments have been short-term (<2 years), performed on saplings and/or in  
84 greenhouses and amongst these very few have included measurements of plant hydraulic  
85 traits or have been located in tropical rainforest environments, with the drought treatment  
86 imposed at hectare-scale affecting hundreds of trees together. Consequently, the capacity of  
87 trees to acclimate to drought, that is to maintain the same performance under drought when  
88 compared to non-droughted conditions, remains highly uncertain, particularly in tropical  
89 rainforest environments.

90 To date, only eight throughfall exclusion experiments (TFE experiments) have been  
91 implemented in tropical forests with reductions in soil moisture imposed for a year or more  
92 (Meir *et al.*, 2015). In a TFE experiment in Sulawesi, after two years of drought, Schuldt *et al.*  
93 (2011) found a reduction in tree hydraulic efficiency, which they suggest might have led  
94 to a reduction in tree growth. This may suggest the hydraulic systems of tropical trees can  
95 respond plastically to drought, but that full acclimation to maintain hydraulic performance  
96 and growth did not occur. In another Asian tropical forest, after four months of TFE in

97 Malaysia (Inoue *et al.*, 2017), leaf turgor loss point had decreased, however, as  
98 photosynthesis was reduced, this also implies substantial acclimation did not occur.  
99 Observations in a TFE experiment in Australia have also shown plastic responses in leaf and  
100 wood anatomical properties linked to hydraulic safety after two years of TFE-imposed  
101 drought, yet similarly no evidence was reported to suggest this led to substantial acclimation  
102 (Tng *et al.*, 2018). In the world's only long-running tropical TFE (15+ years of TFE), in an  
103 Amazonian forest, limited plasticity was found in leaf level anatomical and water relations  
104 traits (Binks *et al.*, 2016) and none in embolism resistance, a key trait controlling hydraulic  
105 safety (Rowland *et al.*, 2015). Studying drought responses over longer time periods is  
106 valuable, particularly given that there is likely to be variation in the responses and types of  
107 adjustments occurring from annual to decadal time periods (da Costa *et al.*, 2014; Meir *et al.*,  
108 2018).

109         Acclimation of a tree's hydraulic system to drought requires adjustments in one or  
110 more key traits to maintain a tree's hydraulic status. The hydraulic status can be evaluated  
111 using hydraulic status variables, such as leaf water potential, hydraulic safety margins or  
112 percentage loss of conductivity in the xylem tissue. These adjustments may confer greater  
113 drought tolerance, for example by increasing xylem resistance to embolism or a greater  
114 capacity to supply water to the leaves when water becomes available, which can occur, as a  
115 consequence by increasing hydraulic conductivity or reducing leaf area to sapwood area  
116 ratio's. (Cruiziat *et al.* 2002; Maseda & Fernandez, 2006; Sperry & Love, 2015). Other  
117 adjustments, such as root system expansion or higher stomatal control, can increase the  
118 capacity to avoid drought by allowing trees to access deeper, wetter soils, or to decouple from  
119 the atmosphere (Delzon *et al.* 2015).

120         Similar processes of acclimation may also be expected as a tree grows. As a tree gets  
121 taller it can be exposed to greater drought stress as it is exposed to higher radiation fluxes, a

122 more desiccating atmosphere and strong winds, alongside having lower leaf water potential  
123 as a consequence of a longer hydraulic path from root to leaf (Kumagai *et al.*, 2001).  
124 Consequently, it should be advantageous for a tree to adjust its hydraulic traits to become  
125 more drought tolerant as it becomes taller. There is evidence of increased hydraulic efficiency  
126 with height for tropical trees (Zach *et al.*, 2010), however Rowland *et al.* (2015a) found that  
127 resistance to embolism decreases as trees get taller. If correct, these results imply that there  
128 are: i) height-related trade-offs, such as changes in hydraulic efficiency, constraining tree  
129 hydraulic safety; and/or ii) large trees over-compensate for the drier canopy environment by  
130 having larger water storage, capacitance and/or deeper roots and/or better water loss control  
131 (Brum *et al.*, 2019), allowing them to down-regulate embolism resistance; or iii) larger trees  
132 are undergoing damage to their hydraulic system, lowering their hydraulic safety (e.g. weaker  
133 pit membranes, due to repeated damage) (Scholz *et al.*, 2007).

134         Constraints or trade-offs in hydraulic traits related to tree height or architecture may  
135 be greater in larger trees, which are close to their maximum height. This may limit their  
136 capabilities to acclimate to drought, potentially explaining why larger trees are more  
137 susceptible to drought-induced mortality in tropical forests and other biomes (McDowell &  
138 Allen, 2015; Bennett *et al.*, 2015; Rowland *et al.*, 2015a; Olson *et al.*, 2018). Drought  
139 experiments in tropical forests have however rarely focussed on tree size effects. The only  
140 existing study investigating how drought responses change with tree size (Rowland *et al.*,  
141 2015) found no interaction between tree size, embolism resistance and a drought treatment.  
142 However, Rowland *et al.* (2015a) were only able to study 6 genera in forest plots containing  
143 94 genera and they only focused on trees which were fully sunlit at their canopy tops. To test  
144 more fully the capacity of tropical forest trees to adjust their hydraulic system to size changes  
145 and to drought, further work is required on a larger number of taxa, spanning multiple tree  
146 size classes and canopy positions.

147 In this study we test the capacity of tropical trees from varying canopy positions to  
148 adjust their hydraulic systems in response to 15 years of experimental TFE and associated  
149 substantial soil moisture deficit. We present measurements of hydraulic traits and hydraulic  
150 status variables (i.e. indicators of the status of a plant's water transport system) linked to  
151 safety and efficiency on >150 individuals of 12 genera, including: resistance to embolism  
152 (xylem water potential causing 50 % and 88% of loss in water transport capacity - P50 and  
153 P88), stem and leaf specific conductivity, leaf to xylem area ratios and leaf minimum  
154 conductance to water vapour (hydraulic traits); and native embolism, pre-dawn and midday  
155 leaf water potential and hydraulic safety margins (hydraulic status). This combination of  
156 hydraulic traits - the mechanistic traits determining a tree's hydraulic functioning - and  
157 hydraulic status variables - the status of a tree's hydraulic system during functioning - allow  
158 us to examine both plasticity (adjustment in hydraulic traits) and acclimation (maintenance  
159 of hydraulic status) following changes in the environment. With this dataset, we test the  
160 following hypotheses:

- 161 1) Tropical trees can acclimate to prolonged soil moisture deficit, by adjusting key  
162 hydraulic traits, to maintain the same plant water status as nearby, cognate, but  
163 non-droughted trees.
- 164 2) Tropical trees acclimate to the negative impacts of long-water transport pathways  
165 and greater exposure to drier atmospheric conditions imposed by increasing tree  
166 height by adjusting key plant hydraulic traits, resulting in different sized trees  
167 having similar water status.
- 168 3) Adjustments in hydraulic traits in response to prolonged soil moisture deficit are  
169 modulated by tree size. We predict that tree size interacts with long-term soil  
170 moisture deficit, such that the capacity to acclimate to soil moisture deficit  
171 decreases with tree size.

172            Additionally, we replicate the analyses of Rowland *et al.* (2015a), which were made at  
173 the same experimental site, testing whether embolism resistance changes with tree size and  
174 across drought-stressed and non-drought-stressed trees, but here we use the much more  
175 extensive sample size and larger dataset acquired in this study.



## 176 **Methods**

### 177 *Site and plant material*

178 Our study site is a tropical lowland rainforest located in the Caxiuanã National Forest,  
179 state of Pará, north-east Brazil (1°43'S, 51°27 W). The site annual rainfall is 2000-2500mm  
180 with a dry season (< 120 mm monthly rainfall) from July to December. A throughfall  
181 exclusion (TFE) experiment was started in 2002, whereby 50% of canopy throughfall is  
182 excluded by a plastic panel structure installed at 1-2m height over a 1 ha area. A 1-2 m trench  
183 was dug in the perimeter of the TFE plot to prevent lateral infiltration of water and all  
184 litterfall falling in the panels is redistributed manually to the soil. The TFE plot is  
185 accompanied by a 1 ha control plot, with a similar perimeter trench but where no throughfall  
186 exclusion has taken place. Both plots have been monitored continuously since 2001; detailed  
187 information on the experiment can be found in ( da Costa *et al.*, 2010; Fisher *et al.*, 2007;  
188 Meir *et al.*, 2015; Rowland *et al.*, 2015b) . In 2016, the TFE caused a mean reduction of 48%  
189 and 56% of soil water content at 10 cm and 100 cm depth, respectively, in the TFE plot  
190 compared to the control plot (Fig. S1).

191 During the peak of the September-October 2016 dry season, we sampled 161 trees  
192 from 12 genera (36 species), 85 from the control plot and 76 from the TFE, with diameters  
193 ranging from 14 to 68 cm at 1.5 m height (sampling details in Table 1 and S1). For each  
194 individual, we collected two branches 1.5 - 2.5 meters long from the top of the canopy. The  
195 branches were fourth to sixth order, counting from the leaves. We collected one set of  
196 branches before sunrise (0400 to 0600 hours) and used them for measures of embolism  
197 resistance and predawn leaf water potential. We collected a second set of branches at midday  
198 (1130 to 1330 hours) and used these for measures of midday leaf water potential, native  
199 embolism, leaf-to-sapwood area, xylem and leaf specific conductivity, minimum leaf

200 conductance and wood density measurements. Immediately after collection, branches were  
201 bagged in thick black plastic sacks with moist paper to humidify internal air and limit leaf  
202 transpiration. Branches were transported 100 m from the plots to measure leaf water  
203 potential, and for the remaining measurements the branches were transported for 30 minutes  
204 to a laboratory. Each day, branches were collected from 6 to 10 different individuals. In all  
205 the branches measured, heartwood was absent and pith area was either absent or negligible.

206 Table 1. Summary of Caxiuanã hydraulic traits and status values for each genus and separately for Control and Throughfall Exclusion (TFE)  
 207 plots. Values presented are mean  $\pm$  SD. Diameter values are maximum and minimum tree diameter at 1.5 m height. Total sample size (i.e.,  
 208 number of individual trees sampled for each trait) is given at the bottom of the table for each trait.

Genus	Plot	Diameter	Hydraulic traits							Hydraulic status			
			P50	P88	K <sub>s</sub>	K <sub>ls</sub>	LS	g <sub>smin</sub>	WD	Ψ <sub>pd</sub>	Ψ <sub>md</sub>	HSMP50	PLC
<i>Aspidosperma</i>	Control	14 to 34	-1.9 $\pm$ 0.38	-3.9 $\pm$ 1.1	3.3 $\pm$ 3.3	0.23 $\pm$ 0.23	13000 $\pm$ 3900	0.068 $\pm$ 0.017	0.61 $\pm$ 0.13	-0.91 $\pm$ 0.35	-2.2 $\pm$ 0.74	-0.083 $\pm$ 0.48	20 $\pm$ 16
	TFE	16 to 32	-3.1 $\pm$ NA	-4.9 $\pm$ NA	0.97 $\pm$ 0.97	0.13 $\pm$ 0.14	7500 $\pm$ 1500	0.081 $\pm$ 0.025	0.59 $\pm$ 0.11	-0.56 $\pm$ 0.35	-1.9 $\pm$ 0.67	0.49 $\pm$ NA	34 $\pm$ 26
<i>Eschweilera</i>	Control	17 to 42	-2.3 $\pm$ 1.1	-4.2 $\pm$ 2.1	4.1 $\pm$ 2.4	0.46 $\pm$ 0.37	11000 $\pm$ 5600	0.089 $\pm$ 0.058	0.64 $\pm$ 0.073	-0.42 $\pm$ 0.11	-1.7 $\pm$ 0.39	0.75 $\pm$ 1	7.6 $\pm$ 2
	TFE	13 to 30	-2.6 $\pm$ 1.1	-4.9 $\pm$ 2.3	5.1 $\pm$ 1.9	0.49 $\pm$ 0.13	11000 $\pm$ 5400	0.076 $\pm$ 0.038	0.65 $\pm$ 0.08	-0.58 $\pm$ 0.14	-2.1 $\pm$ 0.45	0.65 $\pm$ 0.96	18 $\pm$ 13
<i>Inga</i>	Control	15 to 39	-2.6 $\pm$ 0.98	-4.4 $\pm$ 1	6.7 $\pm$ 1.9	0.87 $\pm$ 0.57	12000 $\pm$ 6300	0.11 $\pm$ 0.052	0.71 $\pm$ 0.069	-0.38 $\pm$ 0.16	-1.9 $\pm$ 0.37	0.82 $\pm$ 1.3	14 $\pm$ 11
	TFE	13 to 56	-2.3 $\pm$ 1.2	-4 $\pm$ 1.9	6.8 $\pm$ 3.3	0.66 $\pm$ 0.33	15000 $\pm$ 7100	0.06 $\pm$ 0.037	0.67 $\pm$ 0.12	-0.44 $\pm$ 0.14	-2 $\pm$ 0.2	0.37 $\pm$ 1.2	18 $\pm$ 6.1
<i>Licania</i>	Control	10 to 28	-2 $\pm$ 0.73	-3.5 $\pm$ 2	0.86 $\pm$ 0.51	0.068 $\pm$ 0.03	14000 $\pm$ 3600	0.057 $\pm$ 0.024	0.73 $\pm$ 0.031	-0.29 $\pm$ 0.11	-1.3 $\pm$ 0.27	0.79 $\pm$ 0.66	26 $\pm$ 11
	TFE	11 to 28	-3.2 $\pm$ 0.51	-6.3 $\pm$ 0.93	0.81 $\pm$ 0.85	0.083 $\pm$ 0.051	10000 $\pm$ 4800	0.061 $\pm$ 0.035	0.72 $\pm$ 0.056	-0.32 $\pm$ 0.15	-1.1 $\pm$ 0.29	2.1 $\pm$ 0.69	23 $\pm$ 1.9
<i>Micropholis</i>	Control	18 to 63	-1.2 $\pm$ 0.63	-2.3 $\pm$ 1.2	3.6 $\pm$ 0.41	0.35 $\pm$ 0.15	13000 $\pm$ 8800	0.096 $\pm$ 0.058	0.6 $\pm$ 0.044	-0.52 $\pm$ 0.16	-2.4 $\pm$ 0.88	-2.3 $\pm$ 0.99	11 $\pm$ 6.9
	TFE	14 to 24	-1.1 $\pm$ NA	-1.9 $\pm$ NA	4.4 $\pm$ 1.3	0.2 $\pm$ 0.13	11000 $\pm$ NA	0.034 $\pm$ 0.0067	0.61 $\pm$ 0.062	-1.3 $\pm$ 0.53	-2.2 $\pm$ 0.46	-0.53 $\pm$ NA	6.2 $\pm$ 8.7
<i>Minquartia</i>	Control	12 to 42	-2 $\pm$ 0.89	-3.8 $\pm$ 2.2	2.5 $\pm$ 0.88	0.24 $\pm$ 0.078	11000 $\pm$ 5000	0.079 $\pm$ 0.042	0.71 $\pm$ 0.066	-0.52 $\pm$ 0.16	-1.5 $\pm$ 0.21	0.53 $\pm$ 0.91	19 $\pm$ 7.5
	TFE	13 to 41	-1.3 $\pm$ 0.87	-3.4 $\pm$ 3.5	2.5 $\pm$ 1.4	0.32 $\pm$ 0.13	11000 $\pm$ 4200	0.052 $\pm$ 0.022	0.68 $\pm$ 0.061	-0.61 $\pm$ 0.23	-1.4 $\pm$ 0.27	-0.19 $\pm$ 0.83	21 $\pm$ 17
<i>Pouteria</i>	Control	12 to 59	-2.2 $\pm$ 1.2	-4.6 $\pm$ 2.8	2.9 $\pm$ 1.2	0.52 $\pm$ 0.4	7600 $\pm$ 3900	0.092 $\pm$ 0.049	0.75 $\pm$ 0.12	-0.63 $\pm$ 0.2	-2.2 $\pm$ 0.48	-0.073 $\pm$ 1.2	19 $\pm$ 12
	TFE	10 to 52	-1.4 $\pm$ 0.49	-2.4 $\pm$ 1.4	2.3 $\pm$ 0.74	0.25 $\pm$ 0.21	11000 $\pm$ 4100	0.067 $\pm$ 0.029	0.7 $\pm$ 0.088	-0.92 $\pm$ 0.32	-2.7 $\pm$ 0.82	-1.5 $\pm$ 0.74	18 $\pm$ 15
<i>Protium</i>	Control	11 to 38	-2.3 $\pm$ 0.72	-5.6 $\pm$ 1.7	3.4 $\pm$ 1.7	0.36 $\pm$ 0.15	9900 $\pm$ 4100	0.056 $\pm$ 0.027	0.57 $\pm$ 0.099	-0.65 $\pm$ 0.32	-1.5 $\pm$ 0.44	0.46 $\pm$ 0.63	17 $\pm$ 9.6
	TFE	16 to 38	-2.7 $\pm$ 0.78	-4.4 $\pm$ 1.4	4.3 $\pm$ 1.7	0.55 $\pm$ 0.19	8200 $\pm$ 3700	0.058 $\pm$ 0.03	0.56 $\pm$ 0.098	-0.62 $\pm$ 0.17	-1.7 $\pm$ 0.67	0.91 $\pm$ 1.2	41 $\pm$ 21

<i>Swartzia</i>	Control	22 to 68	-3.1 ± 1.6	-5.8 ± 2.8	5.2 ± 3.1	0.49 ± 0.26	11000 ± 3600	0.11 ± 0.077	0.67 ± 0.038	-0.3 ± 0.067	-2.1 ± 0.52	1.1 ± 1.6	21 ± 16
	TFE	10 to 64	-3.1 ± 1.1	-5.3 ± 1.2	3.1 ± 1.6	0.37 ± 0.2	9400 ± 5700	0.094 ± 0.057	0.72 ± 0.067	-0.46 ± 0.19	-2.2 ± 0.41	0.78 ± 1.4	33 ± 11
<i>Syzygiopsis</i>	Control	14 to 52	-1.4 ± 0.75	-2.2 ± 1	2.8 ± 0.87	0.4 ± 0.24	8000 ± 1900	0.057 ± 0.025	0.55 ± 0.039	-0.7 ± 0.089	-1.8 ± 0.19	-0.38 ± 0.78	15 ± 5.1
	TFE	24 to 59	-1.5 ± 0.74	-3.3 ± 1.9	2.8 ± 0.69	0.47 ± 0.058	6000 ± 730	0.067 ± NA	0.55 ± 0.021	-1 ± 0.6	-2.7 ± 0.72	-1.2 ± 1.5	34 ± NA
<i>Virola</i>	Control	27 to 48	-1.9 ± 1.4	-4.4 ± 3.2	NA	NA	NA	0.047 ± 0.039	0.49 ± NA	-0.65 ± 0.49	-2.4 ± 0.21	-0.42 ± 1.6	NA
	TFE	20 to 35	-1.6 ± 0.85	-3.3 ± 1.6	NA	NA	NA	0.05 ± 0.01	0.5 ± 0.056	-1.1 ± 0.63	-2.5 ± 0.53	-0.95 ± 1.2	NA
<i>Vouacapoua</i>	Control	12 to 56	-3 ± 0.59	-5.7 ± 1.9	2.4 ± 2.2	0.27 ± 0.34	9500 ± 5400	0.088 ± 0.027	0.65 ± 0.093	-0.45 ± 0.11	-2.1 ± 0.73	0.38 ± 1.1	14 ± 8.9
	TFE	15 to 57	-2.6 ± 1.6	-4.4 ± 3.2	3.5 ± 2.5	0.44 ± 0.4	9800 ± 3700	0.064 ± 0.032	0.68 ± 0.11	-0.62 ± 0.14	-2.8 ± 0.79	-0.14 ± 2.3	21 ± 9.5
Total samples			99	99	135	135	135	150	140	159	159	99	135

209

210 P50 and P88- xylem embolism resistance, xylem water potential leading to 50% and 88% of loss in water transport capacity (MPa);  $K_s$  –  
211 maximum hydraulic specific conductivity ( $\text{kg m m}^{-2} \text{s}^{-1} \text{MPa}^{-1}$ );  $K_{ls}$  - maximum hydraulic leaf specific conductivity ( $\text{kg m m}^{-2} \text{s}^{-1} \text{MPa}^{-1}$ ); LS –  
212 leaf to sapwood area ( $\text{m}^2 \text{m}^{-2}$ );  $g_{\text{min}}$  – minimum stomatal conductance ( $\text{mol m}^{-2} \text{s}^{-1}$ ); WD – wood density ( $\text{g cm}^{-3}$ );  $\Psi_{\text{pd}}$  - predawn water potential  
213 (MPa);  $\Psi_{\text{md}}$  – midday water potential (MPa); HSMP50 – hydraulic safety margin to P50 (MPa); PLC – native dry season percentage loss of  
214 conductivity (%).

215 *Predawn and midday water potential*

216 We measured leaf water potential ( $\Psi$ ) in the field immediately after collection using a  
217 pressure chamber (Model 1505, PMS; 0.05 MPa resolution). For each tree we measured  
218 water potential of two leaves, or three leaves if the first two measures differed by more than  
219 0.2 MPa for predawn and 0.4 MPa for midday measurements.

220

221 *Wood density, leaf-to-sapwood area and minimum stomatal conductance*

222 We measured wood density on woody sections 40 to 80 mm long and 4 to 7 mm  
223 diameter cut from the branch. We debarked samples, immersed them in water for 24 hours to  
224 rehydrate and measured saturated volume using the water displacement method (Pérez-  
225 Harguindeguy *et al.*, 2013). We then oven dried the samples at 60°C for 48 hours and  
226 measured their dry weight with a precision scale.

227 We determined leaf to sapwood area ratio (LS), on all branches by measuring leaf  
228 area and calculating sapwood area from two diameter measurements of the debarked basal  
229 part of the branch using precision calipers. We measured leaf area by scanning all leaves on  
230 the branch and quantifying their area using Image J software (version 1.6.0\_20; Schneider *et*  
231 *al.*, 2012). We calculated LS as the total branch leaf area divided by its basal sapwood area.

232 For minimum leaf conductance ( $g_{\text{min}}$ ) we used the leaf conductance to water vapour  
233 measured on the abaxial surface of leaves kept 30 minutes in the dark, using an infrared gas  
234 analyzer (Li-COR 6400, USA). All leaves measured were adult, undamaged, upper canopy  
235 leaves.  $g_{\text{min}}$  is likely a combination of stomatal conductance due to leakage from  
236 partially closed stomata and cuticular conductance.  $g_{\text{min}}$  is part of the dataset presented in  
237 Rowland *et al.* (submitted) and further leaf gas exchange measurement details can be found  
238 therein.

239

240 *Hydraulic efficiency and native embolism*

241 We calculated maximum hydraulic specific conductivity ( $K_s$ ) as a measure of xylem  
242 hydraulic efficiency and maximum leaf specific conductivity ( $K_{ls}$ ) as a measure of leaf water  
243 supply capacity. We used the native percentage loss of conductivity of the collected branches  
244 ( $PLC_{nat}$ ) as a measure of native embolism. To estimate these variables, we measured branch  
245 xylem hydraulic conductivity before and after flushing to remove emboli. We also measured  
246 the leaf area distal to the sample. We used the 1.5 to 2.5 m long branches collected at midday  
247 to measure hydraulic conductivity. We cut 10-15 cm long segments from each branch base  
248 underwater and let them rehydrate for 15 min to release tension and avoid artefacts (Venturas  
249 *et al.*, 2015). Subsequently, to relax the tension in the branch we cut 1-1.5 m of branch from  
250 base to leaves underwater, in steps of ~15 cm, and used the distal end of the branch for  
251 hydraulic measurements, to ensure no artificially embolised vessels were present in the  
252 measured sample. Maximum vessel length, measured on a subsample of 17 branches was  
253  $32.7 \pm 15.2$  cm (55.5 cm maximum), confirming 2 m long branches were sufficient to avoid  
254 open vessel artefacts. All samples used for hydraulic measurements were first or second order  
255 branches, were between 30-55 mm in length and 3-5 mm diameter and were recut underwater  
256 with a sharp razor blade before connecting to the apparatus, to ensure all vessels were open at  
257 both ends. We measured flow using the pressure drop over a capillary method in an hydraulic  
258 apparatus (Sperry *et al.*, 1988; Espino & Schenk, 2011; Pereira & Mazzafera, 2012), where a  
259 capillary of known conductance is connected in series with the sample, and flushing samples  
260 to remove emboli and estimate maximum conductance (Martin-StPaul *et al.*, 2014). We  
261 calculated  $PLC_{nat}$  as the ratio of  $K_{s_{nat}}$  to  $K_s$  multiplied by 100. We calculated  $K_{ls}$  as sample  
262 hydraulic conductivity (i.e. sample conductance times sample length) after flushing divided  
263 by the leaf area distal to the measured sample.

264

265 *Embolism resistance and hydraulic safety*

266 As an index of xylem embolism resistance, we used P50 and P88, the xylem water  
267 potentials where, respectively, 50% and 88% of hydraulic conductivity is lost (Choat *et al.*  
268 2012). We also used P50 to calculate the hydraulic safety margin - the difference between  
269 P50 and  $\Psi_{md}$ , an index of tree hydraulic safety. We measured the xylem embolism resistance  
270 of each branch using the pneumatic method (Pereira *et al.*, 2016; Zhang *et al.*, 2018). With  
271 this method the loss of hydraulic conductance is estimated from the increase in air volume  
272 inside the wood caused by embolism formation, as the branch dehydrates. Air volume is  
273 estimated from the air discharge from the cut end of the branch into a vacuum reservoir (~50  
274 kPa absolute pressure) of known volume during a given amount of time (2.5 minutes; details  
275 in Methods S1 and Bittencourt *et al.*, 2018). We dehydrated branches using the bench  
276 dehydration method. Before each air discharge measurement, we bagged branches for one  
277 hour for leaf and wood xylem water potential to equilibrate. Directly after the air discharge  
278 was measured, we estimated wood xylem water potential by measuring the leaf water  
279 potential of one or two leaves. Drought embolism resistance is then given by the increase in  
280 air discharge (PAD – percentage air discharge) with decreasing xylem water potential for  
281 each tree. To calculate P50, we pooled together the data for the 2-3 branch replicates from the  
282 same tree and fitted a sigmoid curve to the data, where P50 and slope ( $a$ ) are the fitted  
283 parameters (Pammenter & Vander Willigen, 1998) and P88 is predicted from the fitted  
284 model:

$$285 \text{ PAD} = 100 / (1 + \exp(a(\Psi - P50)))$$

286

287 *Data analysis*

288 To test our hypotheses, we evaluated the significance of plot, diameter (a proxy of  
289 tree height and canopy exposure - see Fig. S2 for tree size and canopy exposure relationships  
290 based on the tree light score estimates for both plots), genus and their interactions as variables  
291 affecting hydraulic traits and hydraulic status. We used linear mixed effect models with plot,  
292 diameter and their interaction treated as fixed effects and we tested the random effect of  
293 genus on the intercept of the model and the slope of the independent variable with the fixed  
294 model terms (i.e. plot and diameter). We started with a full fixed and random effect model of  
295 plot, diameter and their interaction and tested the significance of the random effect by  
296 removing it and evaluating if the model significantly worsened. We tested sequentially for the  
297 random effect of genus on: 1) the model intercept; 2) the relationship between the  
298 independent variable and tree diameter and; 3) on the relationship between the independent  
299 variable and plot. The genus effect on plot without effect on intercept produces the same fit  
300 as genus effect on plot and intercept, as plot is a factorial term, so this model was not tested.  
301 When more than one random effect format was significant, we chose the simplest random  
302 effect (i.e. intercept effect only), unless the Akaike Information Criterion of the more  
303 complex model was at least 2 units lower than the simpler model. After testing the random  
304 effects, we tested the fixed effects by first removing the interaction term and testing if this  
305 significantly worsened the model and after this using the same approach with the additive  
306 terms. If no random effect was significant, we changed to a fixed effect model (R base  
307 package “lm” function) and analysed fixed effects in the same way. To be confident in our  
308 capacity to evaluate plasticity/acclimation we also repeated the above analysis at a species  
309 level, instead of genus level. Analysing the data in this way leads to a less balanced sampling  
310 design and a reduction in the replicates available for comparison between the plots, due to  
311 high tropical forest diversity. However, if a comparison of the genus level and species level  
312 analysis delivers the same results it confers confidence in our capacity to demonstrate either



313 full, partial or no drought acclimation through combining a more statistically robust data-set  
314 at the genus-level, with a less robust, but more scale-appropriate analysis at the species level.

315 We also re-tested Rowland *et al.*'s (2015a) relationship between tree size and P50 by  
316 analysing our individual dataset alone (30 samples Control and 32 samples TFE, considering  
317 only the genera in common with Rowland *et al.* (2015a), and then in combination with the  
318 Rowland *et al.* (2015a) dataset (48 samples Control and 51 samples TFE) using fixed effect  
319 models. We use a fixed-effect model for consistency with the analysis carried out in Rowland  
320 *et al.* (2015a). It should be noted that here we use the pneumatic method for determining P50,  
321 whereas Rowland *et al.* (2015a) used the air-injection method and fitted a Weibull, not a  
322 sigmoidal function. Despite the different methods, we find a correlation of 0.95 between P50  
323 estimated from Weibull and Sigmoid functions for our data (Fig. S3). Finally, to test the  
324 effect that species composition of our and the Rowland *et al.* (2015a) data set has on the P50-  
325 tree size relationships and to verify the sensitivity of the results (p-value) to the combination  
326 of genera used, we performed a taxon-sensitivity analysis by deleting one, two, three and four  
327 genera at a time from the full dataset (all 12 genera in this study) for all possible genera  
328 combinations (793 total combinations tested).

329 We used the R programming environment and statistical packages (version 3.3.0; R  
330 Core Team 2016) for all data processing and analysis. We fitted linear mixed effect models  
331 with “lme” function of the nlme package (Pinheiro *et al.* 2014) and linear fixed effect models  
332 with the “lm” function (base packages). We used marginal and conditional pseudo-r<sup>2</sup> to  
333 quantify mixed models relative goodness of fit (function “r.squaredGLMM” of the MuMIn  
334 package; Barton 2016). We followed the guidelines of Zuur *et al.* (2009) and Thomas *et al.*  
335 (2017) for assessing significance of model terms and validating model assumptions. For  
336 mixed effect model terms, we fitted models with restricted maximum likelihood and  
337 calculated a log-likelihood ratio to test if the removal of a term significantly affected the

338 quality of the model in relation to the more complex model in which it was nested. For fixed  
339 effect models, we used the same approach but with an F-test between the model with and the  
340 model without the removed variable. We used the “anova” function (stats package, with  
341 mixed effect model methods from nlme package) for log-likelihood ratio and F tests. If the p  
342 value of the test was less than 0.05, we assumed that the model without the variable was  
343 significantly worse than the model with the variable included. The final model with only  
344 significant terms was refitted with maximum likelihood and we validated model assumptions  
345 using diagnostic plots for normality and homogeneity of residuals and collinearity of  
346 predictors. To identify influential observations, we calculated Cook’s distance and dfbeta for  
347 each dataset using base package functions for linear models and “influence.ME”  
348 (Nieuwenhios *et al.* 2012) package functions for mixed effect models. The embolism  
349 resistance dataset is smaller than the other datasets, as we could not process all collected  
350 samples (Table 1). No hydraulic conductivity data is presented for *Virola* as it clearly  
351 decreased with the duration of the measurement, producing negative percentage loss of  
352 conductance, likely due to the abundance of latex being exuded from the cut end of the  
353 sample. Whenever we had more than one replicate per tree, as for leaf water potential, we  
354 used the tree-level mean of the replicates. We considered significant the probability of the  
355 tested hypothesis versus the null hypothesis (p-value) being lower than 0.05 and marginally  
356 significant when it was between 0.05 and 0.10.

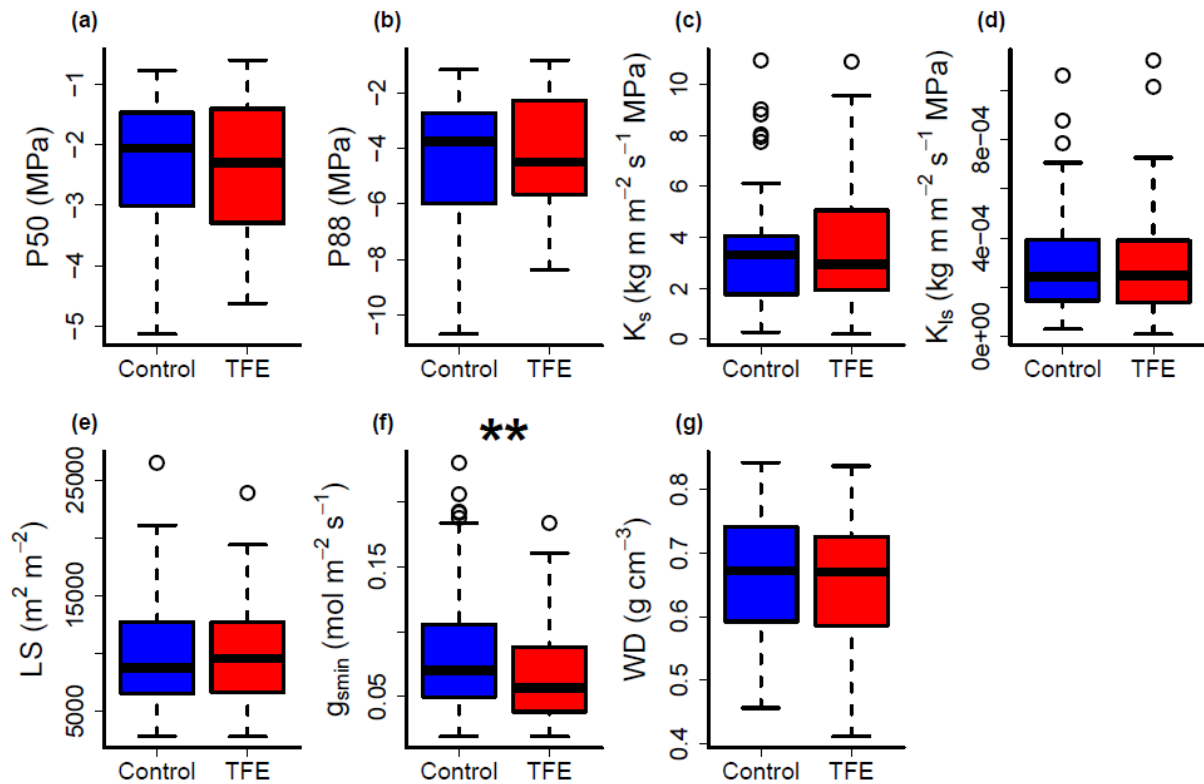
357

## 358 **Results**

### 359 *Throughfall exclusion effects on tree hydraulics*

360 Drought stress caused by 15 years of throughfall exclusion (TFE) had limited effect  
361 on hydraulic traits (Fig. 1; Table 1) Xylem embolism resistance (P50 and P88), specific  
362 conductivity ( $K_s$ ), leaf specific conductivity ( $K_{ls}$ ), leaf to sapwood area (LS) and wood  
363 density (WD) did not change in response to the TFE manipulation (Table 2; Table S2).  
364 Minimum stomatal conductance ( $g_{smin}$ ) was the only trait which adjusted in response to the  
365 TFE ( $p = 0.011$ ), with a decrease of  $0.007 \text{ mol m}^{-2} \text{ s}^{-1}$  (Fig. 1f; all coefficients are presented in  
366 Table S3).

367



368

369 Figure 1. Hydraulic trait responses on trees surviving after 15 years of throughfall exclusion  
 370 (TFE) in Caxiuanã. a-b) P50 and P88 - xylem embolism resistance (MPa); c)  $K_s$  – maximum  
 371 hydraulic specific conductivity ( $\text{kg m m}^{-2} \text{s}^{-1} \text{MPa}$ ); e)  $K_{ls}$  - maximum hydraulic leaf -specific  
 372 conductivity ( $\text{kg m m}^{-2} \text{s}^{-1} \text{MPa}$ ); e) LS – leaf to sapwood area ratio ( $\text{m}^2 \text{m}^{-2}$ ); f)  $g_{smin}$  –  
 373 minimum stomatal conductance ( $\text{mol m}^{-2} \text{s}^{-1}$ ); g) WD – wood density ( $\text{g cm}^{-3}$ ). We consider  
 374 changes in structural hydraulic traits (i.e. plot effect models) as plasticity in response to  
 375 drought. The box represents quartiles 1 and 3, with the central line indicating the median.  
 376 Whiskers are either maximum value or 1.5 interquartile range above the quartile 3, when  
 377 outliers are present. Traits for which plot had a significant effect are marked with \* ( $p <$   
 378 0.05), \*\* ( $p < 0.01$ ) and \*\*\* ( $p < 0.001$ ). P-values are from mixed effects analysis (see Table  
 379 2 for models and analysis section in Methods).

380

381 Table 2. Results of linear mixed effect models of plot (Control versus TFE) and tree diameter effects on hydraulic traits and hydraulic status. The  
 382 combination of the tested random effects is genus effect on intercept only, and/or on plot and diameter slopes (see analysis section in Methods  
 383 for details). Values for fixed effects are fitted parameter  $\pm$  standard error; values for random effects are standard deviation of the normal  
 384 distribution from where coefficients were fitted.  $R^2$  is the full model coefficient of determination (conditional pseudo- $R^2$ ). Random effects  
 385 notation are: 1|genus is a random genus effect on intercept; diameter|genus or plot|genus indicates a random intercept effect plus a random genus  
 386 effect on diameter or plot term (i.e. an interaction term of genus modelled as a random variable with plot or diameter). Plot (i.e. experimental  
 387 treatment) is a two level factor (Control and TFE), with Control as the reference level. Blank cells indicate that the effect is non-significant.

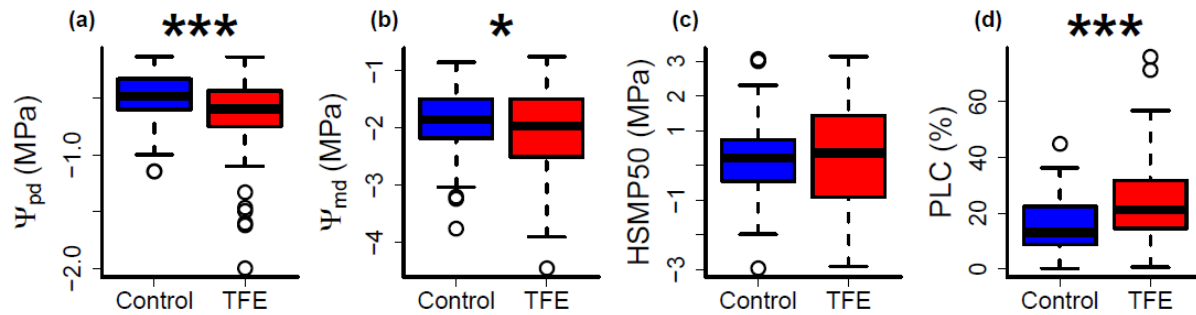
	Fixed effect			Random effects			$R^2$
	Intercept	Plot	Diameter	Genus	Plot Genus	Diameter Genus	
P50	-2.21 $\pm$ 0.16			0.44*			0.16
P88	-4.22 $\pm$ 0.21						0
$K_s$	3.31 $\pm$ 0.48			2.29***		0.065***	0.53
$K_{is}$	0.21 $\pm$ 0.06		0.005 $\pm$ 0.001 **	0.11**			0.26
LS	10266 $\pm$ 439.6						0
$g_{smin}$	0.083 $\pm$ 0.005	-0.018 $\pm$ 0.007**					0.043
WD	0.65 $\pm$ 0.02			0.06***			0.36

Status	$\Psi_{pd}$	$-0.52 \pm 0.05$	$-0.18 \pm 0.07^{***}$	$0.13^{***}$	$0.19^{***}$	0.49
	$\Psi_{md}$	$-1.88 \pm 0.12$	$-0.2 \pm 0.09^*$	$0.38^{***}$		0.35
	HSMP50	$0.14 \pm 0.24$		$0.71^{***}$		0.26
	PLC	$16.2 \pm 2.3$	$8.3 \pm 2.5^{**}$	$5.0^*$		0.2

388 P50 - xylem embolism resistance (MPa);  $\Psi_{pd}$  - predawn water potential (MPa);  $\Psi_{md}$  - midday water potential (MPa); HSMP50 – hydraulic  
389 safety margin to P50 (MPa); PLC – native dry season percentage loss of conductivity (%);  $K_s$  – maximum hydraulic specific conductivity (kg m  
390  $m^{-2} s^{-1} MPa^{-1}$ );  $K_{ls}$  - maximum hydraulic leaf-specific conductivity (kg m  $m^{-2} s^{-1} MPa^{-1}$ ); LS – leaf to sapwood area ratio ( $m^2 m^{-2}$ );  $g_{smin}$  –  
391 minimum stomatal conductance ( $mol m^{-2} s^{-1}$ ); WD – wood density ( $g cm^{-3}$ ).

392 \*  $p < 0.05$ ; \*\*  $p < 0.01$ ; \*\*\*  $p < 0.001$

393           The TFE manipulation had a highly significant effect on all hydraulic status variables  
394 (Fig. 2), except on hydraulic safety margin (HSMP50; Table 2). TFE caused a decrease in  
395 peak dry season  $\Psi_{md}$  of  $-0.19$  MPa ( $p = 0.02$ ) with a high intra-generic variability (SD of  
396  $0.38$  MPa for random genus effect on intercept and an average increase in percentage loss of  
397 conductance of  $8.3\%$  (PLC;  $p = 0.001$ ; see coefficients in Table S3). Predawn water potential  
398 ( $\Psi_{pd}$ ) was affected by the TFE with a reduction of  $-0.18$  MPa ( $p < 0.001$ ), equal to a  $35\%$   
399 decrease relative to control, which was further modulated by random genus-specific effects ( $p$   
400  $< 0.001$ ; Figure 3; see also the following paragraph), leading to a TFE maximum effect of  
401 reducing predawn water potential by  $0.52$  MPa in *Micropholis*.



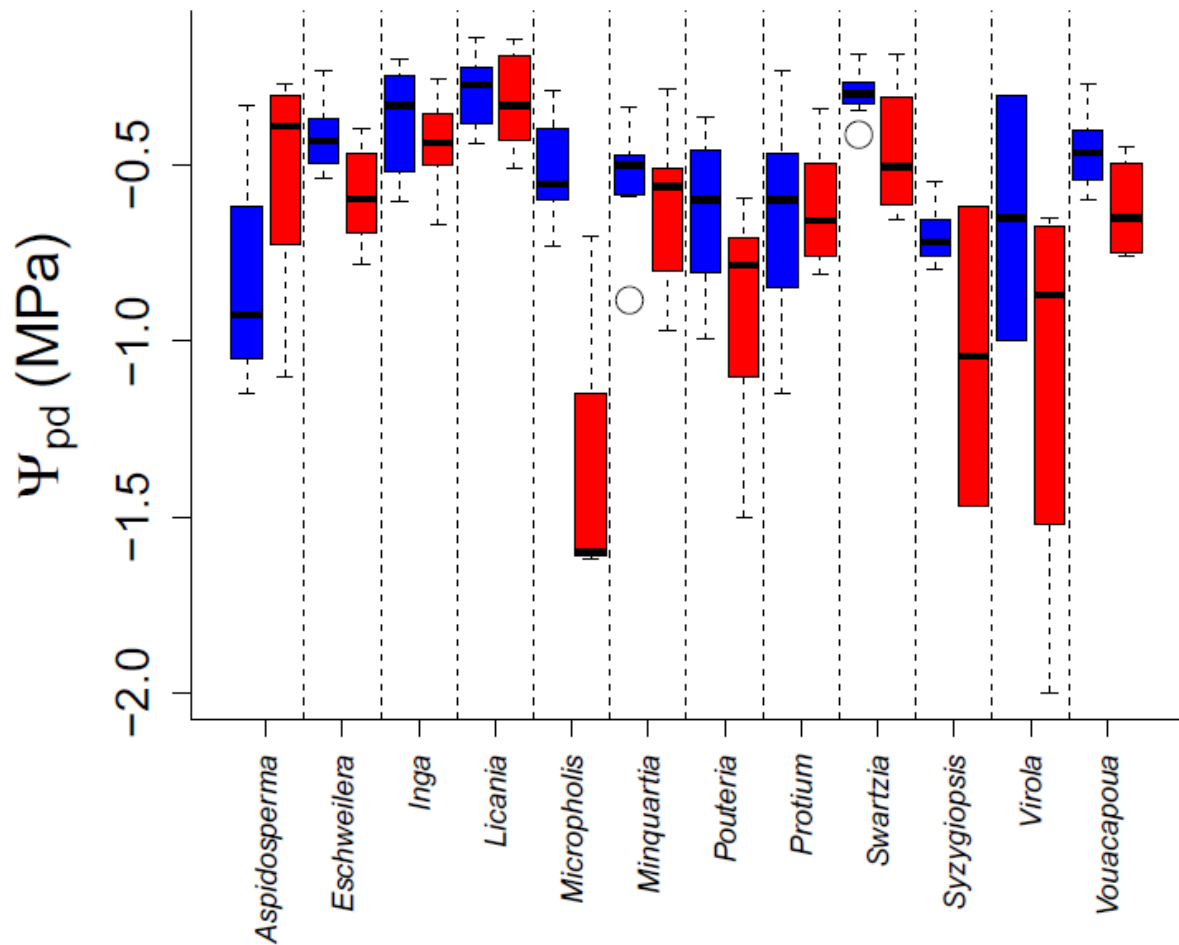
402

403 Figure 2. Hydraulic status of trees surviving after 15 years of throughfall exclusion (TFE) in  
 404 the peak of the dry season in Caxiuanã. a)  $\Psi_{pd}$  - predawn water potential (MPa); b)  $\Psi_{md}$   
 405 midday water potential (MPa); c) HSMP50 – hydraulic safety margin to P50; d) PLC – native  
 406 dry season percentage loss of conductivity (% maximum conductance). We consider  
 407 homeostasis of hydraulic status (i.e. no plot effect) as an indicator of hydraulic acclimation.  
 408 The box represents quartiles 1 and 3, with the central line indicating the median. Whiskers  
 409 are either maximum value or 1.5 interquartile range above the quartile 3, when outliers are  
 410 present. Traits for which plot (i.e. TFE treatment) had a significant effect are marked with \*  
 411 ( $p < 0.05$ ), \*\* ( $p < 0.01$ ) and \*\*\* ( $p < 0.001$ ). P-values are from mixed effects analysis (see  
 412 Table 2 for models and analysis section in Methods).



413 *Tree size effects on hydraulic traits and interaction with TFE*

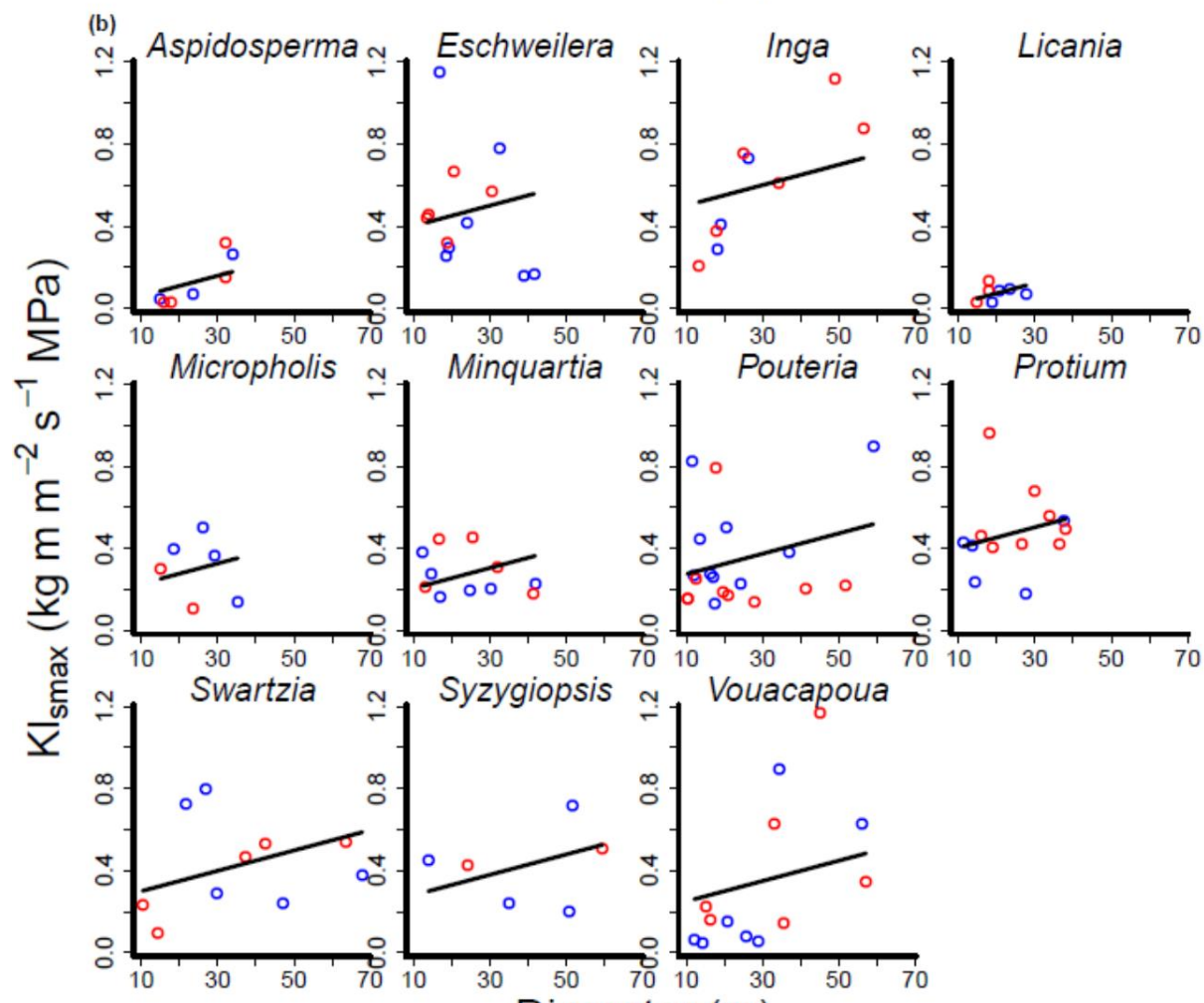
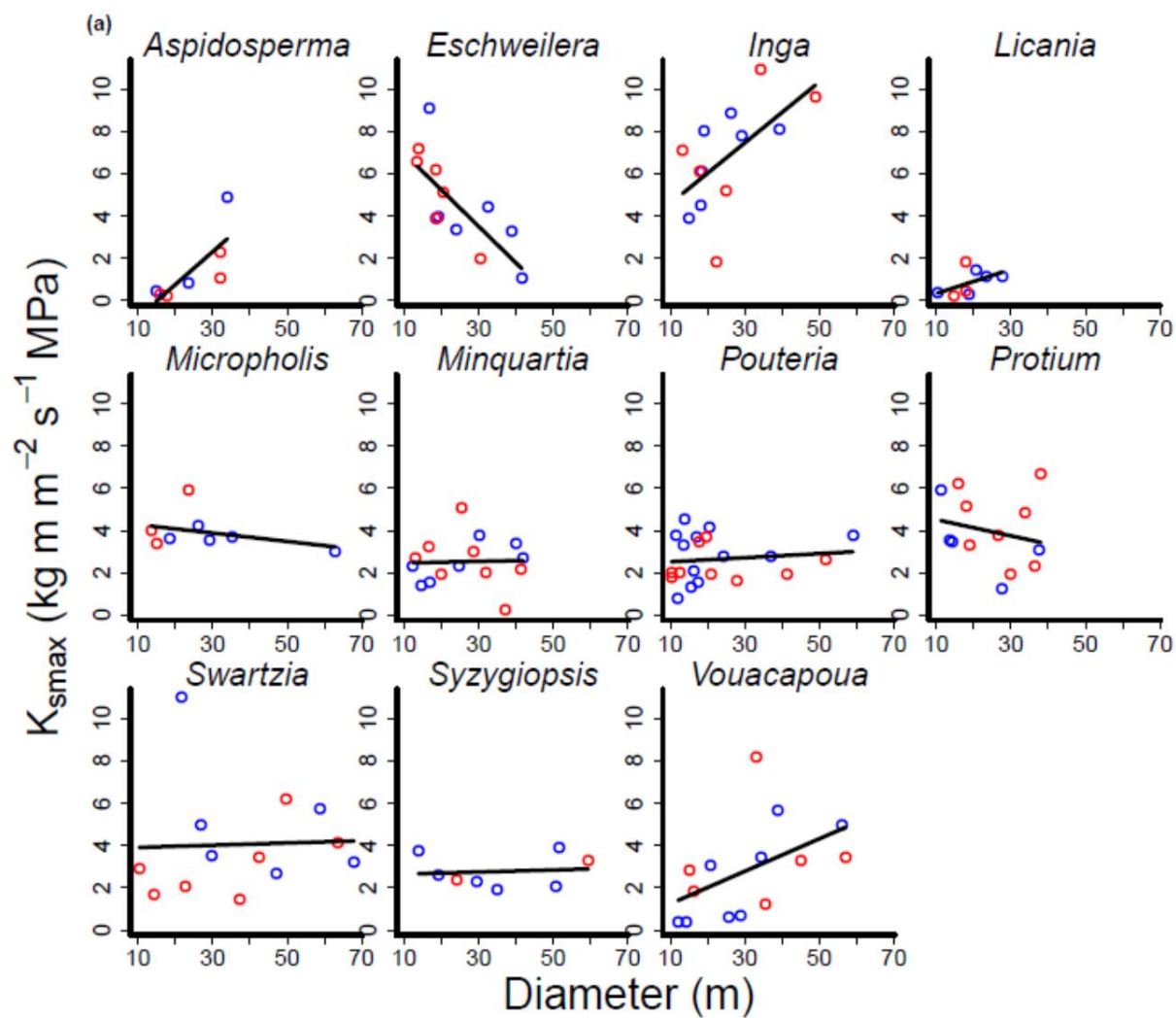
414 Tree stem diameter did not affect hydraulic status and only affected  $K_s$  and  $K_{ls}$  among  
415 the hydraulic traits (Table 2). For  $K_s$ , the effect of increasing diameter was genus-dependent,  
416 as indicated by a significant random genus effect on diameter ( $p < 0.001$ ; Figure 4a; Table 2;  
417 Table S2). The effect of diameter on  $K_s$  was positive for *Inga*, *Aspidosperma* and  
418 *Vouacapoua* while it was negative for *Eschweilera* and close to zero for the other genera  
419 (Fig. 4a and Table S3). For  $K_{ls}$ , stem diameter was significant (Tables 1) however, contrary to  
420  $K_s$ , the effect was not genus dependent (no random genus effect on diameter- $K_{ls}$  relationship),  
421 and  $K_{ls}$  showed a consistent increase with stem diameter (Fig. 4b). The random genus effect  
422 on the diameter-P50 relationship was significant ( $p = 0.035$ ; Table S2; Fig. 5), but was not  
423 the most parsimonious model (AIC of 316 against an AIC of 315.8 for the random intercept  
424 model only). There was no fixed diameter effect on P50 ( $p = 0.29$ , Table S2) but the  
425 interaction effect between diameter and plot was marginally significant ( $p = 0.066$ ; Table S2).  
426 We found no evidence of any interaction of plot and tree stem diameter with hydraulic traits  
427 or with hydraulic status (Table 2 and Table S2).



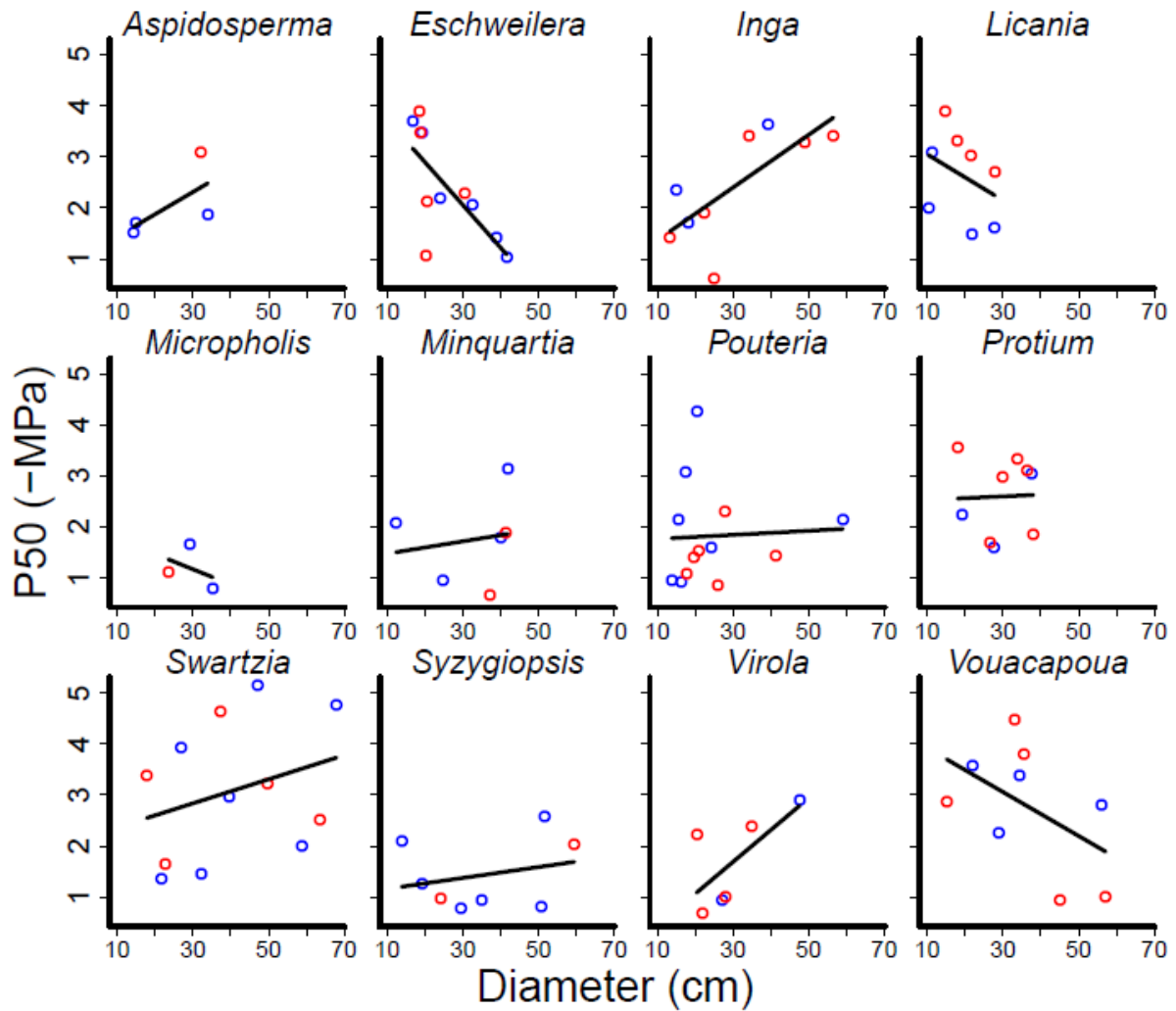
428

429 Figure 3. Throughfall exclusion (TFE) effect on predawn water potential of the studied genus  
 430 ( $\Psi_{pd}$ ), showing the genus specific variation in  $\Psi_{pd}$  response to TFE. TFE had both a fixed  
 431 effect of reducing  $\Psi_{pd}$  and a random effect (genus specific effect) on  $\Psi_{pd}$  (see Table 1). Red  
 432 and blue boxplots are data from the TFE plot and control plots, respectively. The box  
 433 represents quartiles 1 and 3, with the central line indicating the mean. Whiskers are either  
 434 maximum value or 1.5 x interquartile range above the quartile 3, when outliers are present.





437 Figure 4. Diameter effects on xylem specific conductivity ( $K_s$ ; a) and leaf specific  
438 conductivity ( $K_{ls}$ ; b) for each studied genus. Fitted lines show the fitted mixed effects model  
439 (see Table 1 and Results section), modified according to the effect of the random variable  
440 (genus) on either the intercept or the slope of the relationship of diameter to the independent  
441 variable ( $K_s$  or  $K_{ls}$ ). For  $K_s$ , the interaction between diameter and random effect, genus is  
442 significant ( $p < 0.001$ ), resulting in different slopes for each genus. For  $K_{ls}$ , the interaction is  
443 significant ( $p = 0.02$ ) but is not the most parsimonious model (AIC of 40.2 against an AIC of  
444 38.6 for genus effect on intercept only, see Table S2), resulting in vertical shifts of otherwise  
445 parallel lines. Blue and red points are data from Control and TFE plots, respectively.



446

447 Figure 5. Diameter effects on embolism resistance (P50; presented as positive values in –

448 MPa) for each studied genus. We modelled the variables using linear models with diameter,

449 genus and their interaction as fixed effects. The model is marginally significant ( $p = 0.066$ ).

450 The fitted line is the fitted, marginally significant model, for each genus. Blue and red points

451 are data from Control and TFE plots, respectively (there was no plot effect on P50 so data

452 were pooled).

453 *Taxonomic effects on the hydraulic system and their interactions with drought and tree size*

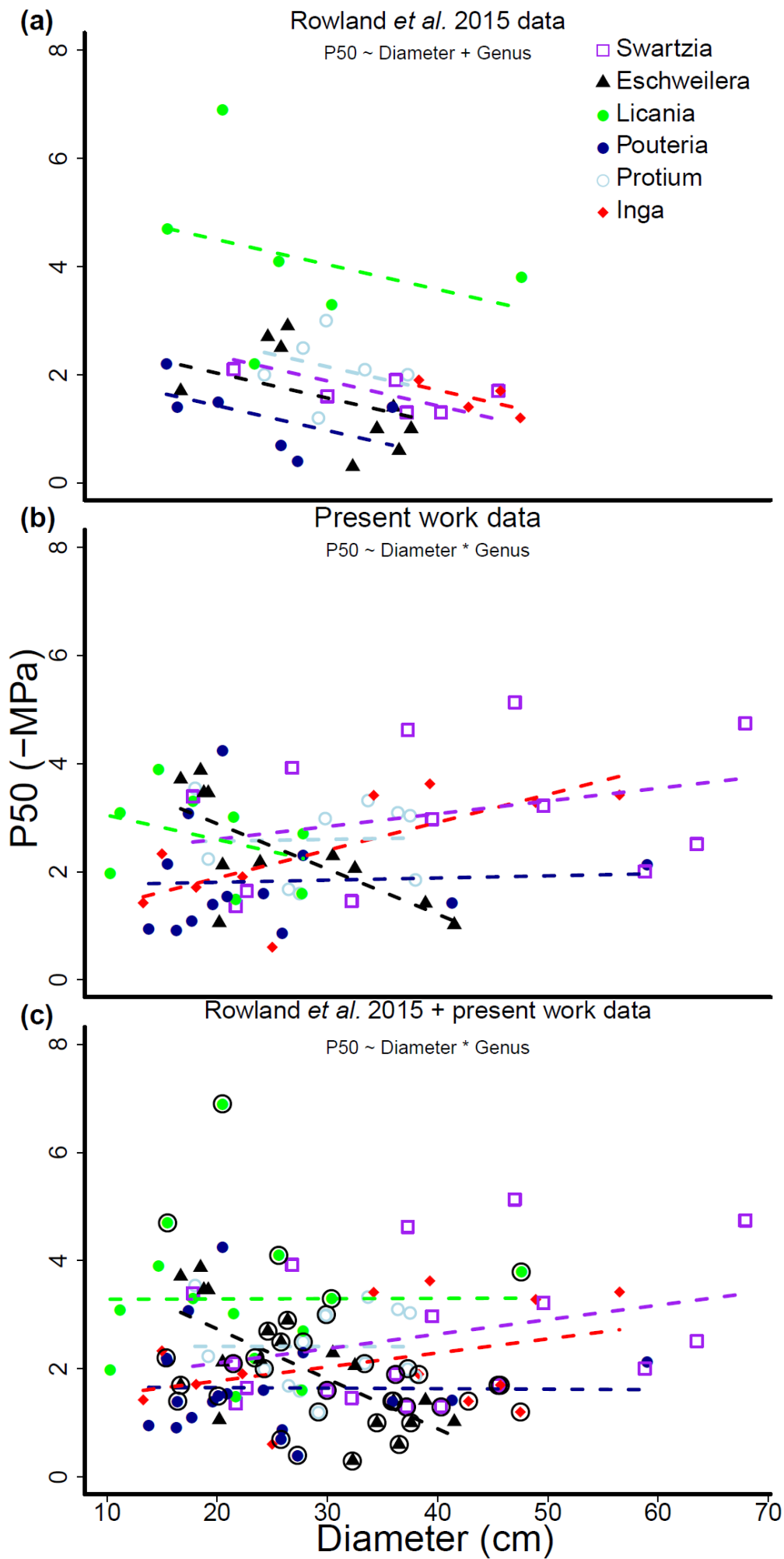
454 Most of the hydraulic traits and hydraulic status variables we measured varied significantly by  
455 genus (Table 2). The form of the taxonomic effect was, except for  $\Psi_{pd}$  and  $K_s$ , an additive  
456 change in intercept with no effect on the plot response (Table 2). Taxonomic effects on  $K_s$   
457 were shown in the previous section. For  $\Psi_{pd}$ , genus-specific effects were evident on the TFE  
458 (Fig. 3). Certain genera demonstrated substantially greater reductions in  $\Psi_{pd}$  in response to  
459 the TFE than others, for example *Micropholis* had a mean decline of -0.43 MPa on the TFE.  
460 When genus was included as a random effect in a MEM for  $\Psi_{pd}$ , with plot as a fixed variable,  
461 it had a SD of 0.19 MPa on the plot- $\Psi_{pd}$  relationship (see interaction coefficients in Table  
462 S3). We could not detect any taxonomic effect on LS, which had a large variability, or on  
463  $g_{smin}$  and P88. When we analysed the data at species level, all the above patterns remained  
464 unchanged (Table S4), except for  $K_s$ , whose random species effect on the diameter slope  
465 could not be detected, and midday water potential, where a random species effect on the plot  
466 effect was now detectable.

467 *Revisiting Rowland et al. (2015)*

468 Rowland *et al.* (2015a) presented the first dataset of P50 for Amazon trees at this site  
469 (reproduced in Fig.6a). We provide here a comparison of the two analyses. Using fixed effect  
470 models, when we analysed the same subset of six genera as analysed by Rowland *et al.*  
471 (2015a), our data also show a significant effect of diameter on P50. However, in our work,  
472 the slope was positive, and not negative as in Rowland *et al.* (2015a), and the interaction  
473 between genus and diameter was also significant ( $p = 0.046$ , Fig. 6b). While *Eschweilera*  
474 presents a strong increase in P50 (less negative values) with diameter, the other genera  
475 showed either a weak decrease in P50 with diameter or an almost negligible diameter effect  
476 (Fig. 6). When the two datasets are combined, the same pattern remains, with P50 being

477 significantly affected by the interaction between diameter and genus and a slightly more  
478 significant diameter effect ( $p = 0.023$ ; Fig. 6c). However, after removal of a single genus  
479 with a strong positive relationship between P50 and diameter (*Eschweilera*) from the  
480 combined datasets, both the diameter interaction with genus and the diameter effect disappear  
481 ( $p = 0.62$  and  $p = 0.14$ ; Fig. S4c). The same occurs if *Eschweilera* is removed from the non-  
482 combined datasets (Fig. S4a and b).





484 Figure 6. Relationship between embolism resistance (P50) and tree diameter using the same  
485 subset of genera as analysed in Rowland *et al.* (2015a). a) The original data and analysis of  
486 Rowland *et al.* (2015a). b) The data from this work only; and c) the combined datasets from  
487 a) and b). Linear fixed-effect models were used in the analysis and the dashed lines are the  
488 fitted model for each genus. In a), diameter and genus were significant while the interaction  
489 term was not. In both b) and c) genus, diameter and their interaction are significant. The  
490 circled data points in c) indicate the 2015 data. As done in Rowland *et al.* (2015a), we display  
491 the Y-axis as the negative of P50 (-P50). The same figure and analysis is presented in Fig. S4  
492 after removing data for *Eschweilera*, the genus with an increase in -P50 with diameter. Note:  
493 P50 values are presented as -MPa, as in (Rowland *et al.*, 2015a).

494           The results from the linear fixed effect models using the Rowland et al (2015a) subset  
495 of the data are partially consistent with the results for this study is full dataset with all 12  
496 genera, whereby a diameter interaction with genus is found to be marginally significant ( $p =$   
497 0.066; Table S2), but this is not the most parsimonious model (AIC of 316 for the random  
498 genus-diameter interaction against an AIC of 315.8 for the simpler genus intercept effect).  
499 We reanalysed the full dataset (all 12 genera in this study) removing one, two, three and four  
500 genera at a time, for all possible genus combinations (793 total combinations tested), to verify  
501 the sensitivity of the results to the combination of genera used. When removing only one  
502 genus at a time, P50 was significantly affected by diameter with a genus interaction 33.3% of  
503 the times and marginally significantly affected 75% of the times. A similar pattern was  
504 observed when two or more genera were removed simultaneously (Fig. S5). This further  
505 supports our finding that the influence of tree diameter on P50 is strongly dependent on the  
506 taxonomic identity of the trees in the dataset, which also strongly influenced whether P50  
507 increased, decreased or did not change with increasing tree size (Fig. S5). On the other hand,  
508 neither the present results nor those of Rowland *et al.* (2015a) show any significant plot (i.e.  
509 treatment) effects on P50.

## 510 Discussion

511 We analysed the effects of a long-term (>15 years) throughfall exclusion experiment  
512 (TFE experiment) on key hydraulic traits and hydraulic status variables, which indicate the  
513 hydraulic stress being experienced by the tree across its water transport system. Despite the  
514 high mortality rates of the largest TFE trees (da Costa et al 2010; Rowland *et al.*, 2015a),  
515 which should have reduced overall inter-tree competition for soil water, soil water content is  
516 significantly lower in the TFE plot relative to the control plot (Fig. S1). This indicates that  
517 competition for water is still high amongst surviving trees and reduced competition following  
518 mortality events has not alleviated soil water stress, which is demonstrated by the observed  
519 lower  $\Psi_{pd}$  and  $\Psi_{md}$  and greater PLC in the droughted trees (Fig. 2). Furthermore, no plasticity  
520 was observed in key hydraulic traits related to hydraulic safety (P50 and P88) and hydraulic  
521 efficiency ( $K_s$ ,  $K_{ls}$ ) in the droughted trees relative to the control, suggesting that tropical trees  
522 may not be able to acclimate their hydraulic systems to long-term drought in order to  
523 maintain the same water status as non-droughted trees, and thus avoid damage to their  
524 hydraulic systems. The high variability in the extent of native embolism and in tissue water  
525 potential among genera supports the hypothesis that some tree groups on the TFE suffer far  
526 greater hydraulic stress than others, which is likely to play a substantial role in triggering the  
527 extensive, genus dependent, drought-induced mortality observed on the plot (da Costa 2010;  
528 Rowland *et al.*, 2015a).

529

### 530 *Plasticity and acclimation to drought in Amazonian trees*

531 Tropical forest drought experiments have reported decreases in hydraulic efficiency (Schuldt  
532 *et al.*, 2011), or no change in embolism resistance (Rowland *et al.*, 2015a) in comparison to  
533 non-droughted, control forest trees. However, shifts in anatomical traits related to hydraulic

534 safety were observed in a TFE experiment located in tropical Australian rainforest (Tng *et al.*,  
535 2018). Our data indicate that in tropical trees exposed to prolonged soil moisture stress,  
536 neither the traits associated with hydraulic safety nor those associated with hydraulic  
537 efficiency adjust to enable acclimation. It is possible that other, unmeasured, traits may be  
538 influencing tree hydraulic status, for example changes in stomatal control and rooting depths.  
539 However, the significantly lower leaf water potential and greater PLC in the TFE trees  
540 suggest other traits, as with our measured traits, are not adjusting sufficiently to allow the  
541 hydraulic system of the droughted trees to acclimate. These patterns which we observe at  
542 genus level remain unchanged when the data are analysed at species level, providing  
543 confidence that acclimation did not occur.

544         Forest resistance and resilience to drought are likely to be mediated by medium and  
545 long-term precipitation variability (Barros *et al.*, 2019; Ciemer *et al.*, 2019), which  
546 themselves influence species distribution patterns at different scales across the Amazon  
547 (Esquivel-Muelbert *et al.*, 2017). Our study site, like much of Amazônia, experiences  
548 relatively small seasonal changes in water availability (Fisher *et al.*, 2008) and it is possible  
549 that species in this region have not evolved significant organ-level plasticity in response to  
550 variability in moisture stress. The capacity of trees to acclimate to drought stress may be  
551 linked to the existing and historical drought stress they experience within an environment  
552 (Zhou, Medlyn, & Prentice, 2016). Therefore, despite a certain degree of seasonality, the lack  
553 of strong rainfall variation, or history of sufficient interannual variance in rainfall at our study  
554 site, may ultimately be responsible for the observed lack of capacity to acclimate.

555         The higher values for PLC in the TFE trees relative to the Control trees, is consistent  
556 with previous studies at this site which suggested that hydraulic impairment is likely to play a  
557 significant role in the much higher levels of drought-induced mortality observed in the TFE  
558 (Rowland *et al.*, 2015a). The higher PLC values in trees in the TFE are likely a consequence

559 of the observed more negative  $\Psi_{pd}$  and  $\Psi_{md}$  (Fig. 2). The mean PLC of the Control trees  
560 during the peak dry season was 16.2%, whereas it was 24.5% on the TFE. Extrapolating from  
561 our PLC results, on average 4.1% of the TFE trees have PLC > 50% while only 1% of  
562 Control trees cross this threshold during the peak dry season (Table 3). However, when  
563 genus-specific effects are considered, the percentage of trees in the TFE crossing the  
564 threshold can be as high as 10.1% for *Protium* trees and as low as 2.1% for *Eschweilera* trees.  
565 Increased PLC under drought is a distinct signal related to tree mortality (Anderegg *et al.*,  
566 2014; Gaylord *et al.*, 2015; Li *et al.*, 2018). While there is no consensus on what PLC level  
567 marks the point of no return from hydraulic failure (Brodribb & Cochard, 2009; Urli *et al.*,  
568 2013), PLCs levels above 50-60 % are very likely to be lethal to trees (Adams *et al.*, 2017).  
569 We note that we did not see a change in the HSMP50 to support the observed changes in  $\Psi$   
570 and PLC. However, we suggest this is because HSMP50 was determined much more by P50  
571 (correlation coefficient of -0.87) than by  $\Psi_{md}$  (correlation coefficient of 0.61).

572         The large variations in PLC which we observed among different genera also confirms  
573 previous observations that drought-induced mortality is more likely for specific groups of  
574 taxa (Esquivel-Muelbert *et al.*, 2017) . According to our models it is unlikely that any  
575 individual tree surviving in the TFE crosses the PLC > 88% threshold in a normal year, such  
576 as when we made our measurements. This suggests that either trees which crossed this  
577 threshold have already died, as such PLC rates are likely to be unsustainable (Adams *et al.*,  
578 2017; Meinzer & McCulloh, 2013), or that such a threshold is only crossed when there is a  
579 particularly intense or long atmospheric drought occurring alongside the soil moisture deficit  
580 caused by the TFE treatment. However, it is also possible that our PLC estimates are an  
581 underestimate as refilling in small branches and leaves, likely related to foliar water uptake  
582 may also occur (Binks *et al.*, 2019).

583 Table 3. Predicted percentage of individuals with PLC > 50% and PLC > 88% in the Control  
 584 and Throughfall Exclusion Experiment (TFE) plots in the peak of the dry season in Caxiuanã.  
 585 Predictions are quantiles with PLC > 50% and 88% of the PLC data distribution fitted with a  
 586 normal variable (PLC ~ N( $\mu$ , SD)). The  $\mu$  (mean) parameter is the genus mean from the  
 587 linear mixed effects model fitted to PLC data (i.e. fixed intercept plus fitted random  
 588 coefficient for the genus; see Table 2 and S2) with or without the TFE effect added. The SD  
 589 (standard deviation) parameter is either assumed to be equal to all groups (SD of all dataset;  
 590 “Constant SD”) or to be taxon-specific (SD of each group).

Genus	Constant SD				Group-specific SD			
	PLC > 50%		PLC > 88%		PLC > 50%		PLC > 88%	
	Control	TFE	Control	TFE	Control	TFE	Control	TFE
All together	1	4.1	0	0	0.1	6.4	0	0
<i>Aspidosperma</i>	1.7	5.9	0	0	3.4	18.7	0	0.9
<i>Eschweilera</i>	0.5	2.1	0	0	0	1.2	0	0
<i>Inga</i>	0.6	2.7	0	0	0	0	0	0
<i>Licania</i>	1.5	5.5	0	0	0.3	0	0	0
<i>Micropholis</i>	0.4	1.7	0	0	0	0	0	0
<i>Minquartia</i>	0.8	3.4	0	0	0	5.5	0	0
<i>Pouteria</i>	0.9	3.6	0	0	0.3	3.7	0	0
<i>Protium</i>	3.3	10.1	0	0	0.3	19	0	0.4
<i>Swartzia</i>	2.2	7.5	0	0	3	3.2	0	0
<i>Syzygiopsis</i>	1.1	4.3	0	0	0	NA	0	NA
<i>Vouacapoua</i>	0.7	3	0	0	0	0.2	0	0

591

592 *Size-related changes in hydraulic plasticity*

593 Given the limited observed plasticity in hydraulic traits between the TFE and Control, we  
594 evaluated how these traits change with tree size and tree canopy exposure, as taller are more  
595 exposed to higher radiation loads and drier atmospheric conditions. Our results demonstrate  
596 plastic responses of some hydraulic traits as trees increase in size, but these responses varied  
597 significantly among genera. Despite these variations, we find no general relationship between  
598 our hydraulic status variables and tree size across all taxa. This may suggest that other,  
599 unmeasured traits, such as whole tree water storage, may be playing a greater role in allowing  
600 these trees to adjust to the high radiation load and drier atmosphere that is experienced higher  
601 up in the canopy, particularly during dry seasons, as discussed above. Variations in  
602 unmeasured traits may also be influencing some of the varying size-hydraulic trait  
603 relationships we observe among taxa.

604         Hydraulic efficiency and leaf water supply efficiency ( $K_s$  and  $K_{ls}$ ) were the traits with  
605 the greatest plasticity associated with tree size. Increases in  $K_s$  are expected as trees grow  
606 taller. To cope with increasing resistance to water flow and drier atmospheric conditions with  
607 increased height, trees may make changes such as increasing the efficiency of water transport  
608 or the investment in xylem tissue, (Bittencourt *et al.*, 2016; Deckmyn, Evans, & Randle,  
609 2006). Vessel diameter, and consequently  $K_s$  of the apex and stem of trees also typically  
610 increases with tree height, allowing  $K_s$  to increase (Olson *et al.*, 2018). Although our data do  
611 show that  $K_s$  changes with tree height, the direction and degree of this change varies  
612 substantially among genera (Fig. 3a). *Inga* and *Eschweilera* had the greatest change in  $K_s$   
613 with stem diameter, however in opposite directions. The other genera showed either very  
614 limited or no plasticity with tree size. These results may be a consequence of  $K_s$  being a  
615 function of multiple structural and anatomical properties (Cruziat *et al.*, 2002; Bittencourt *et*  
616 *al.*, 2016), which may change for other purposes in relation to tree size.



617 We found no evidence of a significant size x plot interaction in structural hydraulic  
618 traits. This contrasts with findings of leaf physiological traits measured on these same trees  
619 where the responses to the drought were modulated by crown exposure to light, and thus tree  
620 height (Rowland *et al.*, in review). Overall, our results suggest that the hydraulic traits we  
621 measured are unlikely to be directly causing the differential drought-induced mortality  
622 observed between small and large trees (da Costa *et al.*, 2010; Nepstad *et al.*, 2007; Phillips *et*  
623 *al.*, 2010). In effect, we could not detect any interaction between tree size and TFE treatment  
624 on response hydraulic traits, suggesting the surviving small and large trees in the TFE are  
625 being equally (negatively) affected by the imposed soil moisture deficit. Either size-  
626 dependent drought effects are related to mechanisms not studied or not captured in our  
627 dataset or they are not reflected in surviving trees. However, we do note that embolism  
628 resistance may contain a genus-dependent interaction with tree size (see next section). If a  
629 taxon that becomes less embolism resistant with increasing size has a large biomass or high  
630 abundance, such as occurs with *Eschweilera*, observed size dependent mortality may be  
631 reflecting taxon-specific patterns, rather than a general community-level pattern.

632

633 *Does embolism resistance change with tree size? Revisiting Rowland et al. (2015)*

634 Rowland *et al.* (2015a) used data from six genera at our study site to demonstrate that  
635 embolism resistance (P50) decreases as tree size increases. This was the first dataset of its  
636 kind for mature Amazonian tropical trees. The limited data available for temperate trees is  
637 inconclusive on direction and strength of this P50 – size relationship (Domec *et al.*, 2009;  
638 Ambrose *et al.*, 2009; Prendin *et al.*, 2018, Olson *et al.*, 2018). Rowland *et al.*, (2015a)  
639 presented these results as evidence that hydraulic failure acts as a trigger of drought-induced  
640 mortality, with a higher mortality risk in taller drought-stressed trees (which had P50 values

641 closer to zero). By subsetting our data to include the same genera, we were able to replicate  
642 this result using different individuals of the same genus and using a different protocol for  
643 hydraulic measurements (Fig. 6), but finding an overall inverse relationship between tree  
644 diameter and P50. However, when data for *Eschweilera* were removed from the analysis, the  
645 relationship between tree size and P50 disappeared (Fig. S4). The data for *Eschweilera* show  
646 a strong decrease in embolism resistance with increasing diameter (Fig. 4). This is relevant  
647 more generally as *Eschweilera coriacea*, one of our sampled species, represents one of the  
648 hyper-dominant trees across the Amazon. It accounts for 5.1% of Amazon trees and 5.5% of  
649 Amazon biomass (Fauset *et al.*, 2015; ter Steege *et al.*, 2013), but which we demonstrate is  
650 highly sensitive to drought when it reaches full stature.

651         Compared to Rowland *et al.* (2015a), our full dataset is comprised of a much larger  
652 number of samples, many more tree species and a wider diameter range, including shaded, or  
653 partially shaded trees. Using this much larger dataset, we found no evidence of a general  
654 decrease in embolism resistance (increasing P50) with tree size. However, we did find  
655 evidence of a marginal tree size effect on P50 interacting with genus identity (Fig. 5),  
656 suggesting that changes in embolism resistance with tree size exist, but are highly dependent  
657 on tree taxonomic identity. Critically, the strength of the P50-tree size relationship was  
658 strongly affected by the subset of data used (Fig. S5). By sequentially removing one or two  
659 genera from our full dataset, we obtained a significant relationship of embolism resistance  
660 with tree size 30% to 50% of the time, respectively. These results indicate that decreases in  
661 embolism resistance with tree size are highly dependent on the combination of genera  
662 analysed and, at least based on our extensive sampling at this site, particularly on the  
663 presence of *Eschweilera* (which has a strong P50-size relationship). Future studies conducted  
664 in highly diverse systems should incorporate taxon-sensitivity analyses.

665           In summary, we tested whether hydraulic traits in Amazon rainforest trees can  
666 acclimate to prolonged soil moisture deficit, and if this adjustment varies with tree size. We  
667 found low plasticity in hydraulic traits in response to prolonged soil drought. This prevented  
668 acclimation in water use from occurring and led to higher levels of hydraulic impairment in  
669 the xylem of some of the droughted trees, suggesting hydraulic impairment is likely to  
670 contribute directly to the drought-induced mortality observed at this site for some genera. In  
671 contrast, we observed some plasticity in hydraulic traits with tree size, but found the plasticity  
672 to be heavily genus-dependent, possibly related to mechanisms allowing acclimation to the  
673 drier atmospheric environment that a tree's canopy experiences as it grows taller. This study  
674 provides new insights into how Amazon rainforest trees may respond to future climate  
675 changes, and suggests overall that their capacity to acclimate may be low. However,  
676 critically, we also show that taxonomic diversity is likely to play an important and complex  
677 role in determining forest-wide hydraulic strategies, acclimation potential and trait  
678 relationships, leading to taxon dependent impacts of climate changes and, possible changes in  
679 forest composition.

680

**681 Acknowledgments**

682 This work was a product of a UK NERC independent fellowship grant NE/N014022/1 to LR.  
683 We recognize the Brazilian Higher Education Coordination Agency (CAPES) scholarships to  
684 PRLB, ALG, PBC and FB. We thank the Royal Society for a Newton International  
685 Fellowship (NF170370) grant to P.R.L.B. This work was also supported by a UK NERC  
686 grant NE/J011002/1 to PM and MM and EU FP7-Amazalert grant to PM, CNPQ grant  
687 457914/2013-0/MCTI/CNPq/FNDCT/LBA/ESECAFLOR to ACLD, and an ARC grant  
688 DP170104091 to PM and FAPESP/Microsoft research (grant 11/52072-0) awarded to RSO.  
689 DCB is supported by a NERC studentship NE/L002434/1. We also thank the UNICAMP  
690 postgraduate programs in Ecology and Plant Biology and the Brazilian Higher Education Co-  
691 ordination Agency (CAPES) for scholarships to PBC, PRLB and ALG. We have no conflict  
692 of interest to declare.

693 **Author Contributions**

694 PRLB, RSO, MM, PM and LR conceived the research ideas, developed the project and wrote  
695 the manuscript. PM and ACLD conceived of and run the experiment. LAG, IC, BPC, DB,  
696 SSV, LVF, AR, AAR, JASJ, LR and PRLB contributed to data collection and all authors  
697 contributed to manuscript preparation.

698 **Data accessibility**

699 The data that support the findings of this study will be openly available in 2021 at the NERC  
700 Centre for Environmental Data Analysis (<http://eidc.ceh.ac.uk/>) with all data collection  
701 funded by UK NERC independent fellowship grant NE/N014022/1.

702

703 **References**

- 704 Adams, H. D., Zeppel, M. J. B., Anderegg, W. R. L., Hartmann, H., Landhäusser, S. M.,  
705 Tissue, D. T., ... McDowell, N. G. (2017). A multi-species synthesis of physiological  
706 mechanisms in drought-induced tree mortality. *Nature Ecology & Evolution*, *1*(9), 1285–  
707 1291. <https://doi.org/10.1038/s41559-017-0248-x>
- 708 Ambrose, A. R., Sillett, S. C., & Dawson, T. E. (2009). Effects of tree height on branch  
709 hydraulics, leaf structure and gas exchange in California redwoods. *Plant, Cell &*  
710 *Environment*, *32*(7), 743–757. <https://doi.org/10.1111/j.1365-3040.2009.01950.x>
- 711 Anderegg, W. R. L., Anderegg, L. D. L., Berry, J. A., & Field, C. B. (2014). Loss of whole-  
712 tree hydraulic conductance during severe drought and multi-year forest die-off. *Oecologia*,  
713 *175*(1), 11–23. <https://doi.org/10.1007/s00442-013-2875-5>
- 714 Awad, H., Barigah, T., Badel, E., Cochard, H., & Herbette, S. (2010). Poplar vulnerability to  
715 xylem cavitation acclimates to drier soil conditions. *Physiologia Plantarum*.  
716 <https://doi.org/10.1111/j.1399-3054.2010.01367.x>
- 717 Barros, F. de V., Bittencourt, P. R. L., Brum, M., Restrepo-Coupe, N., Pereira, L., Teodoro,  
718 G. S., ... Oliveira, R. S. (2019). Hydraulic traits explain differential responses of Amazonian  
719 forests to the 2015 El Niño-induced drought. *New Phytologist*, *223*(3), 1253–1266.  
720 <https://doi.org/10.1111/nph.15909>
- 721 Barton K. (2016). MuMIn: multi-model inference. [https://cran.r-](https://cran.r-project.org/web/packages/MuMIn/index.html)  
722 [project.org/web/packages/MuMIn/index.html](https://cran.r-project.org/web/packages/MuMIn/index.html).
- 723 Beikircher, B., & Mayr, S. (2009). Intraspecific differences in drought tolerance and  
724 acclimation in hydraulics of *Ligustrum vulgare* and *Viburnum lantana*. *Tree Physiology*,  
725 *29*(6), 765–775. <https://doi.org/10.1093/treephys/tpp018>

- 726 Bennett, A. C., McDowell, N. G., Allen, C. D., & Anderson-Teixeira, K. J. (2015). Larger  
727 trees suffer most during drought in forests worldwide. *Nature Plants*, *1*(10), 15139.  
728 <https://doi.org/10.1038/nplants.2015.139>
- 729 Binks, O., Meir, P., Rowland, L., da Costa, A. C. L., Vasconcelos, S. S., de Oliveira, A. A.  
730 R., ... Mencuccini, M. (2016). Plasticity in leaf-level water relations of tropical rainforest  
731 trees in response to experimental drought. *New Phytologist*, *211*(2), 477–488.  
732 <https://doi.org/10.1111/nph.13927>
- 733 Binks, O., Mencuccini, M., Rowland, L., Costa, A. C. L., Carvalho, C. J. R., Bittencourt, P.,  
734 ... Meir, P. (2019). Foliar water uptake in Amazonian trees: Evidence and consequences.  
735 *Global Change Biology*. <https://doi.org/10.1111/gcb.14666>
- 736 Bittencourt, P., Pereira, L., & Oliveira, R. (2018). Pneumatic Method to Measure Plant  
737 Xylem Embolism. *BIO-PROTOCOL*, *8*(20). <https://doi.org/10.21769/BioProtoc.3059>
- 738 Bittencourt, P. R., Pereira, L., & Oliveira, R. S. (2016). On xylem hydraulic efficiencies,  
739 wood space-use and the safety–efficiency tradeoff. *New Phytologist*, *211*(4), 1152–1155.
- 740 Brodribb, T. J., & Cochard, H. (2009). Hydraulic Failure Defines the Recovery and Point of  
741 Death in Water-Stressed Conifers. *PLANT PHYSIOLOGY*, *149*(1), 575–584.  
742 <https://doi.org/10.1104/pp.108.129783>
- 743 Brum, M., Vadeboncoeur, M. A., Ivanov, V., Asbjornsen, H., Saleska, S., Alves, L. F., ...  
744 Oliveira, R. S. (2019). Hydrological niche segregation defines forest structure and drought  
745 tolerance strategies in a seasonal Amazon forest. *Journal of Ecology*, *107*(1), 318–333.  
746 <https://doi.org/10.1111/1365-2745.13022>
- 747 Choat, B., Brodribb, T. J., Brodersen, C. R., Duursma, R. A., López, R., & Medlyn, B. E.  
748 (2018). Triggers of tree mortality under drought. *Nature*, *558*(7711), 531–539.  
749 <https://doi.org/10.1038/s41586-018-0240-x>



- 750 Christoffersen, B. O., Gloor, M., Fauset, S., Fyllas, N. M., Galbraith, D. R., Baker, T. R., ...  
751 Meir, P. (2016). Linking hydraulic traits to tropical forest function in a size-structured and  
752 trait-driven model (TFS v.1-Hydro). *Geoscientific Model Development Discussions*, 1–60.  
753 <https://doi.org/10.5194/gmd-2016-128>
- 754 Ciemer, C., Boers, N., Hirota, M., Kurths, J., Müller-Hansen, F., Oliveira, R. S., &  
755 Winkelmann, R. (2019). Higher resilience to climatic disturbances in tropical vegetation  
756 exposed to more variable rainfall. *Nature Geoscience*, 12(3), 174–179.  
757 <https://doi.org/10.1038/s41561-019-0312-z>
- 758 Corlett, R. T. (2016). The Impacts of Droughts in Tropical Forests. *Trends in Plant Science*,  
759 21(7), 584–593. <https://doi.org/10.1016/j.tplants.2016.02.003>
- 760 Cruiziat, P., Cochard, H., & Améglio, T. (2002). Hydraulic architecture of trees: Main  
761 concepts and results. *Annals of Forest Science*, 59(7), 723–752.
- 762 da Costa, Antonio C. L., Rowland, L., Oliveira, R. S., Oliveira, A. A. R., Binks, O. J.,  
763 Salmon, Y., ... Meir, P. (2018). Stand dynamics modulate water cycling and mortality risk in  
764 droughted tropical forest. *Global Change Biology*, 24(1), 249–258.  
765 <https://doi.org/10.1111/gcb.13851>
- 766 da Costa, Antonio Carlos Lola, Galbraith, D., Almeida, S., Portela, B. T. T., da Costa, M., de  
767 Athaydes Silva Junior, J., ... Meir, P. (2010). Effect of 7 yr of experimental drought on  
768 vegetation dynamics and biomass storage of an eastern Amazonian rainforest. *New*  
769 *Phytologist*, 187(3), 579–591. <https://doi.org/10.1111/j.1469-8137.2010.03309.x>
- 770 da Costa, Antonio C.L., Metcalfe, D. B., Doughty, C. E., de Oliveira, A. A. R., Neto, G. F.  
771 C., da Costa, M. C., ... Malhi, Y. (2014). Ecosystem respiration and net primary productivity  
772 after 8–10 years of experimental through-fall reduction in an eastern Amazon forest. *Plant*  
773 *Ecology & Diversity*, 7(1–2), 7–24. <https://doi.org/10.1080/17550874.2013.798366>

- 774 Dayer, S., Peña, J. P., Gindro, K., Torregrosa, L., Voinesco, F., Martínez, L., ... Zufferey, V.  
775 (2017). Changes in leaf stomatal conductance, petiole hydraulics and vessel morphology in  
776 grapevine (*Vitis vinifera* cv. Chasselas) under different light and irrigation regimes.  
777 *Functional Plant Biology*, 44(7), 679. <https://doi.org/10.1071/FP16041>
- 778 Deckmyn, G., Evans, S. P., & Randle, T. J. (2006). Refined pipe theory for mechanistic  
779 modeling of wood development. *Tree Physiology*, 26(6), 703–717.
- 780 Domec, J.-C., Warren, J. M., Meinzer, F. C., & Lachenbruch, B. (2009). Safety Factors for  
781 Xylem Failure by Implosion and Air-Seeding Within Roots, Trunks and Branches of Young  
782 and Old Conifer Trees. *IAWA Journal*, 30(2), 101–120. [https://doi.org/10.1163/22941932-](https://doi.org/10.1163/22941932-90000207)  
783 [90000207](https://doi.org/10.1163/22941932-90000207)
- 784 Delzon S. (2015). New insight into leaf drought tolerance. *Functional Ecology* 29: 1247–  
785 1249.
- 786 Donovan, L. A., Richards, J. H., & Linton, M. J. (2003). Magnitude and Mechanisms of  
787 Disequilibrium between Predawn Plant and Soil Water Potentials. *Ecology*, 84(2), 463–470.
- 788 Duffy, P. B., Brando, P., Asner, G. P., & Field, C. B. (2015). Projections of future  
789 meteorological drought and wet periods in the Amazon. *Proceedings of the National*  
790 *Academy of Sciences*, 112(43), 13172–13177.
- 791 Egea, G., González-real, M. M., Baille, A., Nortes, P. A., Conesa, M. R., & Ruiz-salleres, I.  
792 (2012). Effects of water stress on irradiance acclimation of leaf traits in almond trees. *Water*,  
793 450–463. <https://doi.org/10.1093/treephys/tps016>
- 794 Eller, C., de V. Barros, F., R.L. Bittencourt, P., Rowland, L., Mencuccini, M., & S. Oliveira,  
795 R. (2018). Xylem hydraulic safety and construction costs determine tropical tree growth: Tree  
796 growth vs hydraulic safety trade-off. *Plant, Cell & Environment*.  
797 <https://doi.org/10.1111/pce.13106>
- 798 Espino, S., & Schenk, H. J. (2011). Mind the bubbles: Achieving stable measurements of  
799 maximum hydraulic conductivity through woody plant samples. *Journal of Experimental*  
800 *Botany*, 62(3), 1119–1132. <https://doi.org/10.1093/jxb/erq338>

801 Esquivel-Muelbert, A., Baker, T. R., Dexter, K. G., Lewis, S. L., ter Steege, H., Lopez-  
802 Gonzalez, G., ... Phillips, O. L. (2017). Seasonal drought limits tree species across the  
803 Neotropics. *Ecography*, *40*(5), 618–629. <https://doi.org/10.1111/ecog.01904>

804 Fauset, S., Johnson, M. O., Gloor, M., Baker, T. R., Monteagudo M., A., Brienens, R. J. W.,  
805 ... Phillips, O. L. (2015). Hyperdominance in Amazonian forest carbon cycling. *Nature*  
806 *Communications*, *6*, 6857. <https://doi.org/10.1038/ncomms7857>

807 Fisher, R. A., Williams, M., da COSTA, A. L., Malhi, Y., da COSTA, R. F., Almeida, S., &  
808 Meir, P. (2007). The response of an Eastern Amazonian rain forest to drought stress: Results  
809 and modelling analyses from a throughfall exclusion experiment. *Global Change Biology*,  
810 *13*(11), 2361–2378. <https://doi.org/10.1111/j.1365-2486.2007.01417.x>

811 Fisher, Rosie A., Williams, M., de Lourdes Ruivo, M., de Costa, A. L., & Meir, P. (2008).  
812 Evaluating climatic and soil water controls on evapotranspiration at two Amazonian  
813 rainforest sites. *Agricultural and Forest Meteorology*, *148*(6–7), 850–861.  
814 <https://doi.org/10.1016/j.agrformet.2007.12.001>

815 Galbraith, D., Levy, P. E., Sitch, S., Huntingford, C., Cox, P., Williams, M., & Meir, P.  
816 (2010). Multiple mechanisms of Amazonian forest biomass losses in three dynamic global  
817 vegetation models under climate change. *New Phytologist*, *187*(3), 647–665.  
818 <https://doi.org/10.1111/j.1469-8137.2010.03350.x>

819 Gaylord, M. L., Kolb, T. E., & McDowell, N. G. (2015). Mechanisms of piñon pine mortality  
820 after severe drought: A retrospective study of mature trees. *Tree Physiology*, *35*(8), 806–816.  
821 <https://doi.org/10.1093/treephys/tpv038>

822 Ghalambor, C. K., McKAY, J. K., Carroll, S. P., & Reznick, D. N. (2007). Adaptive versus  
823 non-adaptive phenotypic plasticity and the potential for contemporary adaptation in new  
824 environments. *Functional Ecology*, *21*(3), 394–407. [https://doi.org/10.1111/j.1365-](https://doi.org/10.1111/j.1365-2435.2007.01283.x)  
825 [2435.2007.01283.x](https://doi.org/10.1111/j.1365-2435.2007.01283.x)

- 826 Inoue, Y., Ichie, T., Kenzo, T., Yoneyama, A., Kumagai, T., & Nakashizuka, T. (2017).  
827 Effects of rainfall exclusion on leaf gas exchange traits and osmotic adjustment in mature  
828 canopy trees of *Dryobalanops aromatica* (Dipterocarpaceae) in a Malaysian tropical rain  
829 forest. *Tree Physiology*, 37(10), 1301–1311. <https://doi.org/10.1093/treephys/tpx053>
- 830 Kattge, J., Díaz, S., Lavorel, S., Prentice, I. C., Leadley, P., BöNisch, G., ... Wirth, C.  
831 (2011). TRY - a global database of plant traits: TRY - A GLOBAL DATABASE OF PLANT  
832 TRAITS. *Global Change Biology*, 17(9), 2905–2935. [https://doi.org/10.1111/j.1365-](https://doi.org/10.1111/j.1365-2486.2011.02451.x)  
833 [2486.2011.02451.x](https://doi.org/10.1111/j.1365-2486.2011.02451.x)
- 834 Kumagai, T., Kuraji, K., Noguchi, H., Tanaka, Y., Tanaka, K., & Suzuki, M. (2001). Vertical  
835 profiles of environmental factors within tropical rainforest, Lambir Hills National Park,  
836 Sarawak, Malaysia. *Journal of Forest Research*, 6(4), 257–264.
- 837 Li, X., Blackman, C. J., Rymer, P. D., Quintans, D., Duursma, R. A., Choat, B., ... Tissue, D.  
838 T. (2018). Xylem embolism measured retrospectively is linked to canopy dieback in natural  
839 populations of *Eucalyptus piperita* following drought. *Tree Physiology*, 38(8), 1193–1199.  
840 <https://doi.org/10.1093/treephys/tpy052>
- 841 Lopes, A. V., Chiang, J. C. H., Thompson, S. A., & Dracup, J. A. (2016). Trend and  
842 uncertainty in spatial-temporal patterns of hydrological droughts in the Amazon basin:  
843 Hydrological Droughts in the Amazon. *Geophysical Research Letters*, 43(7), 3307–3316.  
844 <https://doi.org/10.1002/2016GL067738>
- 845 Malhi, Y., Aragão, L. E., Galbraith, D., Huntingford, C., Fisher, R., Zelazowski, P., ... Meir,  
846 P. (2009). Exploring the likelihood and mechanism of a climate-change-induced dieback of  
847 the Amazon rainforest. *Proceedings of the National Academy of Sciences*, 106(49), 20610–  
848 20615.
- 849 Marengo, J. A., Souza, C. M., Thonicke, K., Burton, C., Halladay, K., Betts, R. A., ... Soares,  
850 W. R. (2018). Changes in Climate and Land Use Over the Amazon Region: Current and

- 851 Future Variability and Trends. *Frontiers in Earth Science*, 6.  
852 <https://doi.org/10.3389/feart.2018.00228>
- 853 Martin-StPaul, N. K., Longepierre, D., Huc, R., Delzon, S., Burlett, R., Joffre, R., ...  
854 Cochard, H. (2014). How reliable are methods to assess xylem vulnerability to cavitation?  
855 The issue of 'open vessel' artifact in oaks. *Tree Physiology*, 34(8), 894–905.  
856 <https://doi.org/10.1093/treephys/tpu059>
- 857 Maseda, P. H., & Fernandez, R. J. (2006). Stay wet or else: Three ways in which plants can  
858 adjust hydraulically to their environment. *Journal of Experimental Botany*, 57(15), 3963–  
859 3977. <https://doi.org/10.1093/jxb/erl127>
- 860 McDowell, N. G., & Allen, C. D. (2015). Darcy's law predicts widespread forest mortality  
861 under climate warming. *Nature Climate Change*, 5(7), 669–672.  
862 <https://doi.org/10.1038/nclimate2641>
- 863 Meinzer, F. C., & McCulloh, K. A. (2013). Xylem recovery from drought-induced embolism:  
864 Where is the hydraulic point of no return? *Tree Physiology*, 33(4), 331–334.  
865 <https://doi.org/10.1093/treephys/tpt022>
- 866 Meir, P., Mencuccini, M., Binks, O., da Costa, A. L., Ferreira, L., & Rowland, L. (2018).  
867 Short-term effects of drought on tropical forest do not fully predict impacts of repeated or  
868 long-term drought: Gas exchange versus growth. *Philosophical Transactions of the Royal  
869 Society B: Biological Sciences*, 373(1760), 20170311. <https://doi.org/10.1098/rstb.2017.0311>
- 870 Meir, P., Wood, T. E., Galbraith, D. R., Brando, P. M., Da Costa, A. C. L., Rowland, L., &  
871 Ferreira, L. V. (2015). Threshold Responses to Soil Moisture Deficit by Trees and Soil in  
872 Tropical Rain Forests: Insights from Field Experiments. *BioScience*, 65(9), 882–892.  
873 <https://doi.org/10.1093/biosci/biv107>
- 874 Mencuccini, M., Manzoni, S., & Christoffersen, B. (2019). Modelling water fluxes in plants:  
875 From tissues to biosphere. *New Phytologist*. <https://doi.org/10.1111/nph.15681>

- 876 Messier, J., McGill, B. J., Enquist, B. J., & Lechowicz, M. J. (2017). Trait variation and  
877 integration across scales: Is the leaf economic spectrum present at local scales? *Ecography*,  
878 *40*(6), 685–697. <https://doi.org/10.1111/ecog.02006>
- 879 Nepstad, D. C., Tohver, I. M., Ray, D., Moutinho, P., & Cardinot, G. (2007). Mortality of  
880 large trees and lianas following experimental drought in an Amazon forest. *Ecology*, *88*(9),  
881 2259–2269.
- 882 Nieuwenhuis R, te Grotenhuis M, Pelzer B. (2012). Influence.ME: tools for detecting  
883 influential data in mixed effects models. *R Journal* *4*, 38.47.
- 884 Olson, M. E., Soriano, D., Rosell, J. A., Anfodillo, T., Donoghue, M. J., Edwards, E. J., ...  
885 Méndez-Alonzo, R. (2018). Plant height and hydraulic vulnerability to drought and cold.  
886 *Proceedings of the National Academy of Sciences*, *115*(29), 7551–7556.  
887 <https://doi.org/10.1073/pnas.1721728115>
- 888 Pammenter, N. W., & Vander Willigen, C. (1998). A mathematical and statistical analysis of  
889 the curves illustrating vulnerability of xylem to cavitation. *Tree Physiology*, *18*(8\_9), 589–  
890 593.
- 891 Pereira, L., Bittencourt, P. R. L., Oliveira, R. S., Junior, M. B. M., Barros, F. V., Ribeiro, R.  
892 V., & Mazzafera, P. (2016). Plant pneumatics: Stem air flow is related to embolism - new  
893 perspectives on methods in plant hydraulics. *New Phytologist*, n/a-n/a.  
894 <https://doi.org/10.1111/nph.13905>
- 895 Pereira, L., & Mazzafera, P. (2012). A low cost apparatus for measuring the xylem hydraulic  
896 conductance in plants. *Bragantia*, *71*(4), 583–587.
- 897 Pérez-Harguindeguy, N., Díaz, S., Garnier, E., Lavorel, S., Poorter, H., Jaureguiberry, P., ...  
898 Cornelissen, J. H. C. (2013). New handbook for standardised measurement of plant  
899 functional traits worldwide. *Australian Journal of Botany*, *61*(3), 167.  
900 <https://doi.org/10.1071/BT12225>

- 901 Phillips, O. L., Van Der Heijden, G., Lewis, S. L., López-González, G., Aragão, L. E., Lloyd,  
902 J., ... others. (2010). Drought–mortality relationships for tropical forests. *New Phytologist*,  
903 187(3), 631–646.
- 904 Pinheiro J, Bates D, DebRoy S, Sarkar D, R Core Team (2014). Nlme: Linear and Nonlinear  
905 Mixed Effects Models. R package version 3.1-118. [http://CRAN.R-](http://CRAN.R-project.org/package=nlme)  
906 [project.org/package=nlme](http://CRAN.R-project.org/package=nlme).
- 907 Powell, T. L., Wheeler, J. K., de Oliveira, A. A. R., da Costa, A. C. L., Saleska, S. R., Meir,  
908 P., & Moorcroft, P. R. (2017). Differences in xylem and leaf hydraulic traits explain  
909 differences in drought tolerance among mature Amazon rainforest trees. *Global Change*  
910 *Biology*, 23(10), 4280–4293. <https://doi.org/10.1111/gcb.13731>
- 911 Prendin, A. L., Mayr, S., Beikircher, B., von Arx, G., & Petit, G. (2018). Xylem anatomical  
912 adjustments prioritize hydraulic efficiency over safety as Norway spruce trees grow taller.  
913 *Tree Physiology*, 38(8), 1088–1097. <https://doi.org/10.1093/treephys/tpy065>
- 914 R Core Team (2016). R: a language and environment for statistical computing. R Foundation  
915 for Statistical Computing, Vienna, Austria. <https://www.R-project.org/>.
- 916 Rowland, L., da Costa, A. C. L., Galbraith, D. R., Oliveira, R. S., Binks, O. J., Oliveira, A. A.  
917 R., ... Meir, P. (2015a). Death from drought in tropical forests is triggered by hydraulics not  
918 carbon starvation. *Nature*. <https://doi.org/10.1038/nature15539>
- 919 Rowland, Lucy, Lobo-do-Vale, R. L., Christoffersen, B. O., Melém, E. A., Kruijt, B.,  
920 Vasconcelos, S. S., ... Meir, P. (2015b). After more than a decade of soil moisture deficit,  
921 tropical rainforest trees maintain photosynthetic capacity, despite increased leaf respiration.  
922 *Global Change Biology*, 21(12), 4662–4672. <https://doi.org/10.1111/gcb.13035>
- 923 Schneider C. A., Rasband W. S., & Eliceiri K. W. (2012). NIH Image to ImageJ: 25 years of  
924 image analysis. *Nature methods* 9(7), 671–675.

- 925 Scholz, F. G., Bucci, S. J., Goldstein, G., Meinzer, F. C., Franco, A. C., & Miralles-Wilhelm,  
926 F. (2007). Biophysical properties and functional significance of stem water storage tissues in  
927 Neotropical savanna trees. *Plant, Cell & Environment*, 30(2), 236–248.  
928 <https://doi.org/10.1111/j.1365-3040.2006.01623.x>
- 929 Schuldt, B., Leuschner, C., Horna, V., Moser, G., Köhler, M., van Straaten, O., & Barus, H.  
930 (2011). Change in hydraulic properties and leaf traits in a tall rainforest tree species subjected  
931 to long-term throughfall exclusion in the perhumid tropics. *Biogeosciences*, 8(8), 2179–2194.  
932 <https://doi.org/10.5194/bg-8-2179-2011>
- 933 Smith, N. G., & Dukes, J. S. (2013). Plant respiration and photosynthesis in global-scale  
934 models: Incorporating acclimation to temperature and CO<sub>2</sub>. *Global Change Biology*, 19(1),  
935 45–63. <https://doi.org/10.1111/j.1365-2486.2012.02797.x>
- 936 Sperry, J. S., Donnelly, J. R., & Tyree, M. T. (1988). A method for measuring hydraulic  
937 conductivity and embolism in xylem. *Plant, Cell and Environment*, 11(1), 35–40.  
938 <https://doi.org/10.1111/j.1365-3040.1988.tb01774.x>
- 939 Sperry, John S., & Love, D. M. (2015). What plant hydraulics can tell us about responses to  
940 climate-change droughts. *New Phytologist*, 207(1), 14–27. <https://doi.org/10.1111/nph.13354>
- 941 Sterck, F., Anten, N. P. R., Schieving, F., & Zuidema, P. A. (2016). Trait Acclimation  
942 Mitigates Mortality Risks of Tropical Canopy Trees under Global Warming. *Frontiers in*  
943 *Plant Science*, 7. <https://doi.org/10.3389/fpls.2016.00607>
- 944 ter Steege, H., Pitman, N. C. A., Sabatier, D., Baraloto, C., Salomao, R. P., Guevara, J. E., ...  
945 Silman, M. R. (2013). Hyperdominance in the Amazonian Tree Flora. *Science*, 342(6156),  
946 1243092–1243092. <https://doi.org/10.1126/science.1243092>
- 947 Thomas R, Lello J, Medeiros R, Pollard A, Robinson P, Seward A, Smith J, Vafidis J,  
948 Vaughan I (2017). Data analysis with R Statistical Software: a guidebook for scientists. Eco-  
949 Explore, United Kindgom.



- 950 Tng, D. Y. P., Apgaua, D. M. G., Ishida, Y. F., Mencuccini, M., Lloyd, J., Laurance, W. F.,  
951 & Laurance, S. G. W. (2018). Rainforest trees respond to drought by modifying their  
952 hydraulic architecture. *Ecology and Evolution*. <https://doi.org/10.1002/ece3.4601>
- 953 Tomasella, M., Beikircher, B., Häberle, K.-H., Hesse, B., Kallenbach, C., Matyssek, R., &  
954 Mayr, S. (2018). Acclimation of branch and leaf hydraulics in adult *Fagus sylvatica* and *Picea*  
955 *abies* in a forest through-fall exclusion experiment. *Tree Physiology*, *38*(2), 198–211.  
956 <https://doi.org/10.1093/treephys/tpx140>
- 957 Urli, M., Porte, A. J., Cochard, H., Guengant, Y., Burlett, R., & Delzon, S. (2013). Xylem  
958 embolism threshold for catastrophic hydraulic failure in angiosperm trees. *Tree Physiology*,  
959 *33*(7), 672–683. <https://doi.org/10.1093/treephys/tpt030>
- 960 Venturas, M. D., Mackinnon, E. D., Jacobsen, A. L., & Pratt, R. B. (2015). Excising stem  
961 samples underwater at native tension does not induce xylem cavitation: No evidence for a  
962 tension-cutting artefact. *Plant, Cell & Environment*, *38*(6), 1060–1068.  
963 <https://doi.org/10.1111/pce.12461>
- 964 Way, D. A., & Yamori, W. (2014). Thermal acclimation of photosynthesis: On the  
965 importance of adjusting our definitions and accounting for thermal acclimation of respiration.  
966 *Photosynthesis Research*, *119*(1–2), 89–100. <https://doi.org/10.1007/s11120-013-9873-7>
- 967 Yue, X., Zuo, X., Yu, Q., Xu, C., Lv, P., Zhang, J., ... Smith, M. D. (2019). Response of  
968 plant functional traits of *Leymus chinensis* to extreme drought in Inner Mongolia grasslands.  
969 *Plant Ecology*, *220*(2), 141–149. <https://doi.org/10.1007/s11258-018-0887-2>
- 970 Zach, A., Schuldt, B., Brix, S., Horna, V., Culmsee, H., & Leuschner, C. (2010). Vessel  
971 diameter and xylem hydraulic conductivity increase with tree height in tropical rainforest  
972 trees in Sulawesi, Indonesia. *Flora - Morphology, Distribution, Functional Ecology of Plants*,  
973 *205*(8), 506–512. <https://doi.org/10.1016/j.flora.2009.12.008>

- 974 Zhang, Y., Lamarque, L. J., Torres-Ruiz, J. M., Schuldt, B., Karimi, Z., Li, S., ... Jansen, S.  
975 (2018). Testing the plant pneumatic method to estimate xylem embolism resistance in stems  
976 of temperate trees. *Tree Physiology*. <https://doi.org/10.1093/treephys/tpy015>
- 977 Zhou, S.-X., Medlyn, B. E., & Prentice, I. C. (2016). Long-term water stress leads to  
978 acclimation of drought sensitivity of photosynthetic capacity in xeric but not riparian  
979 *Eucalyptus* species. *Annals of Botany*, 117(1), 133–144. <https://doi.org/10.1093/aob/mcv161>
- 980 Zuur A, Ieno E, Walker N, Saveliev A Smith G. (2009). *Mixed Effects Models and*  
981 *Extensions in Ecology with R*. New York, US. Springer Verlag